

CHALMERS



DESIGN OF STEERING WHEEL FORCE FEEDBACK SYSTEM WITH FOCUS ON LANE KEEPING ASSISTANCE APPLIED IN DRIVING SIMULATOR

Master's Thesis in the Systems control and Mechatronics

Abolfazl Tahmasebi Inallu

Department of Signals and Systems
Division of Automatic control, Automation and Mechatronics
Mechatronics group
CHALMERS UNIVERSITY OF TECHNOLOGY
Göteborg, Sweden 2014
Master's thesis 2014: EX063/2014

MASTER'S THESIS IN SYSTEMS CONTROL AND MECHATRONICS

**DESIGN OF STEERING WHEEL FORCE FEEDBACK SYSTEM WITH
FOCUS ON LANE KEEPING ASSISTANCE APPLIED IN DRIVING
SIMULATOR**

Systems control and Mechatronics

Abolfazl Tahmasebi Inallu

Department of Signals and Systems
Division of Automatic control, Automation and Mechatronics
Mechatronics group
CHALMERS UNIVERSITY OF TECHNOLOGY
Göteborg, Sweden 2014

DESIGN OF STEERING WHEEL FORCE FEEDBACK SYSTEM WITH FOCUS ON LANE KEEPING ASSISTANCE APPLIED IN DRIVING SIMULATOR

Systems control and Mechatronics

Abolfazl Tahmasebi Inallu

© ABOLFAZL TAHMASEBI INALLU 2014

Master's Thesis 2014: EX063/2014

ISSN 1652-8557

Department of Signals and Systems

Division of Automatic control, Automation and Mechatronics

Mechatronics group

Chalmers University of Technology

SE-412 96 Göteborg

Sweden

Cover:

Chalmers driving Simulator which was used in this project

Repro service / Department of Signals and Systems

Göteborg, Sweden 2014

DESIGN OF STEERING WHEEL FORCE FEEDBACK SYSTEM WITH FOCUS ON LANE KEEPING ASSISTANCE APPLIED IN DRIVING SIMULATOR

Master's Thesis in the Systems control and Mechatronics
Abolfazl Tahmasebi Inallu
Department of Signals and Systems
Division of *Automatic control, Automation and Mechatronics*
Mechatronics group
Chalmers University of Technology

ABSTRACT

In recent years driving simulators are being widely used by automotive manufactures and researchers especially related in Human-In-The Loop (HIL) experiments. Simulators help researchers reduce prototyping time and cost. Simulators provide unlimited parameterization, more safety and enhanced repeatability. They play an important role in studies of the driver's behaviour in unstable vehicle conditions and manoeuvres.

The goal of this thesis is to create a more real steering feeling for drivers in simulators. Increasing the reality of the steering enhance the driving experience on simulator. The work is divided into two parts; the first part is development of a steering wheel force feedback and the second part is development of a Lane Keeping Assistance System (LKAS), where the steering wheel force feedback system is a component. The steering force feedback system developed includes effect of the kingpin and caster angles on tire forces and self-aligning torque, which have been shown to be important factors for realizing good steering feeling.

In the second part an LKAS is proposed, the idea is to apply an assistance torque depending of lateral offset and heading error in order to minimize trajectory overshoot. The calculated lane keeping assistance torque is added to the steering system feedback torque. Chalmers simulator is used to evaluate the proposed steering force feedback system and the LKAS. The simulator results demonstrate that the LKAS reduces lateral offset of a vehicle and driver's need to interfere with the system and that the steering feeling is improved.

Key words: Steering Wheel feedback torque, driving simulator, lane-keeping assisting

TABLE OF CONTENTS

	<u>Page</u>
TABLE OF CONTENTS	V
1. INTRODUCTION	1
1.1 Chalmers driving simulator	1
1.1.1 Computing component	1
1.1.2 Software for the simulator	2
1.1.3 Motion hardware	2
1.2 Master thesis's goal	4
1.3 Model characteristics	5
1.4 Model limitations	5
2. VEHICLE DYNAMICS MODEL	7
2.1 VDM structure of XC90 Volvo used in this report	7
2.2 Coordinate systems	9
2.3 Model inputs and outputs	11
2.4 Model terminology	13
2.5 Tire modelling	14
2.5.1 TMEasy tire model	16
2.5.2 Longitudinal forces	16
2.5.3 Lateral force	17
2.5.4 Self-aligning torque	19
2.6 Vehicle model	21
2.6.1 Equations of motion	21
3. STEERING SYSTEM MODELING	23
3.1 Steering system overview	23
3.2 Mathematical modelling of steering system	29
3.2.1 Steering system forces and moments	30
3.2.2 Mathematical modelling of tire forces	32
3.2.3 Mathematical modelling of steering column	35
3.3 Friction torque modelling	37
3.4 Power steering modelling	38
4. LANE-KEEPING ASSISTANCE SYSTEM	43
4.1 Lane-keeping controller	44
4.1.1 Vehicle-road model	45
4.1.2 Lane-departure prevention controller	48
4.2 Modelling of force feedback generation for lane-keeping assistance torque	51

5. STEERING WHEEL FORCE FEEDBACK IMPLEMENTATION ON DRIVING SIMULATOR	53
5.1 PWM generation	54
5.2 Steering wheel feedback torque command	59
6. MODEL VALIDATION	61
6.1 Comparison model with measurement data	61
6.2 Steering response evaluating in driving simulator	63
6.3 Tests for evaluating the lane keeping assistance torque functionality in driving simulator	66
7. CONCLUSION	69
8. RECOMMENDATION AND FUTURE WORK	70
REFERENCES	71
APPENDICES	73
APPENDIX A	74
APPENDIX B	75
APPENDIX C	77
APPENDIX D	80

Preface

This Master's thesis was carried out from October 2012 to December 2013 at the Department of Signals and Systems at Chalmers University of Technology and Electronics department of Istanbul Technical University.

This work wouldn't have been possible without the enormous support provided by my supervisor, **Jonas Fredriksson**, who supported me all the time during the thesis. I would like to thank **Jonas Sjöberg**, research group leader of Mechatronics group for his support in relation to driving simulator equipment problems.

I would also thank my advisor in Istanbul Technical University, **Dr. Müştak Erhan Yalçın** who gave me the opportunity to work on my thesis at Chalmers University of Technology.

I also would like to thank my friends **Alberto Morando**, **Artem Kusachov**, **Faouzi Al Mouatamid**, **Gonçalo Salazar**, **Pontus Petersson**, for helping me during the implementation of model on the driving simulator.

My greatest appreciation and friendship goes to my closest friends, **Mohammad Kazem Hosseini** and **Toumaj Kohandel**, who was always a great support in all my struggles during my life.

Finally I owe special thanks to my girlfriend, **Faezeh Navvab** who supported me, I will never forget it!

Göteborg January 2014

Abolfazl Tahmasebi Inallu

Notations

\mathbf{a}_y	Lateral acceleration
\mathbf{a}_x	Longitudinal acceleration
\mathbf{a}_z	Vertical acceleration
$\mathbf{A}_{\text{Servo}}$	Area of the piston in the servo assistance cylinder
\mathbf{b}_r	Rack damping coefficient
\mathbf{b}_s	Steering Wheel damping coefficient
\mathbf{b}_{TB}	Torsion bar damping
\mathbf{C}_f	Front tires cornering stiffness
\mathbf{C}_r	Rear tires cornering stiffness
$\mathbf{C}_{\text{servo}}$	Steering servo assistance
\mathbf{CF}	Dahl model coulomb friction level
\mathbf{D}	Steering wheel and column damping
\mathbf{D}_{rack}	Rack damping
\mathbf{F}_{Long}	Longitudinal force of front left and right tires
\mathbf{F}_{Lat}	Lateral force of front left and right tires
\mathbf{F}_p	Force acting on the pinion
\mathbf{F}_r	Force on the rack
$\mathbf{F}_{\text{rolling } i}$	Rolling resistance force at wheel i .
\mathbf{F}_{yf}	Lateral force of front tire
\mathbf{F}_{yr}	Lateral force of rear tire
$\mathbf{F}_{\text{Servo}}$	Servo assistance force
\mathbf{FL}	Front left
\mathbf{FR}	Front right
\mathbf{FX}_i	Total tire force in longitudinal direction
\mathbf{FY}_i	Total tire force in lateral direction
\mathbf{FZ}_i	Total tire force in vertical direction
\mathbf{J}_{sw}	Steering wheel moment of inertia.
\mathbf{J}_z	Vehicle moment of inertia with respect to z axis.
\mathbf{K}_s	Steering wheel stiffness constant
\mathbf{K}_{TB}	Torsion bar stiffness constant

l	Vehicle length
L_{arm}	Steering arm lever length
l_f	Distance between front tire and COG
l_r	Distance between rear tire and COG
m	Vehicle mass
M_Z	Self-aligning torque
r_p	Pinion radius
r_{KP}	Scrub radius
R	Radius of tire
Rl	Rear left
R_{nom}	Tire nominal radius.
RR	Rear right
S	Longitudinal tire slip
u	Longitudinal velocity of COG
v	Lateral velocity of COG
V_x	Longitudinal velocity of vehicle
V_y	Lateral velocity of vehicle
x_r	Rack displacement
\dot{x}_r	Rack velocity
γ	King pin angle
θ_{sw}	Steering wheel angle
δ	Steering angle
σ	Dahl stiffness coefficient
$\psi, \dot{\psi}$	Yaw angle and yaw rate
τ	Torque
θ_p	Pinion angle
β	Side slip angle
$\alpha_{f,r}$	Front and rear tire slip angle
ω	Rotational velocity

1. INTRODUCTION

Driving simulators are being increasingly used by automotive manufactures for investigation of vehicle systems and driver's behaviour in different situations. A simulator allow us to investigate e.g. how the driver reacts to new active safety technologies such as lane keeping assist, stability control system, etc.

This thesis describes the modelling and development of a steering wheel force feedback system in Simulink[®] for a driving simulator. The goal is to mimic a real vehicle's steering feeling, and also to investigate how steering support systems can be developed and evaluated.

For this reason, the model is combined of steering wheel feedback torque with the lane keeping assistance torque in a new model of steering system dynamics to assist driver and support him to keep the vehicle between the road limits.

1.1 Chalmers driving simulator

A driving simulator is a useful tool for conducting driving experiments. They are mainly used for research purposes in the area of human factors as they provide a safe and cheap way for repeatability and unlimited parameterization testing of new technologies to be implemented in vehicles. A driving simulator consists of 3 main parts: Computing component, Software for the simulator, Motion hardware. The overall architecture of Chalmers simulator is shown in Figure 1.1 and Figure 1.2. Belows follows a description of Chalmers driving simulator.

1.1.1 Computing component

Chalmers driving simulator consists of a Real-time National Instruments (NI) computer (NI PXI_8110) that is responsible for interfacing with the environment via two boards: Analog-to-Digital boards and Digital-Analog boards. A computer called the "Kernel" is responsible for running a scenario of experiment and takes care of interactions between the host and the backup computers. The host PC runs Matlab[®]/Simulink[®] where the vehicle model and the control algorithms are implemented. The host PC sends a car model to Real-Time computer which runs it

and sends the car state interaction to Kernel. The Kernel sends the received information (car's positions, accelerations, speeds...) to another computer called gateway/backup computer. Basically, the motion platform is controlled by these four computers.

1.1.2 Software for the simulator

Software from Matlab[®]/ Simulink[®] and NI Veristand (Lab View) is used for the operation of the simulator. The vehicle dynamics is configured in Matlab[®]/ Simulink[®] model, with 14 DOF (Degree Of Freedom) model which has been developed as a master thesis by Benito& Nilsson in Chalmers at 2006. All characteristics of the model such as constants and relevant information has been derived to reasonable a *Volvo XC90* specification. It incorporates steering geometry, vehicle control, powertrain, brakes, wheels, suspension dynamics, steering system model, chassis, etc. The Vehicle Dynamics Model (VDM) is being executed at 1 kHz at the "slave" board.

1.1.3 Motion hardware

The driving simulator can render inertial and steering feel through the motion platform and the Force Feedback Steering Wheel (FFSW) respectively. The motion platform consists of two main parts: Cockpit, where the driver is seated and a Moog Stewart platform. The cockpit consists of a quarter of a Volvo S80, which is mounted on an electrically powered six degree of freedom Stewart platform and provides the interaction between the driver and the vehicle system. The Moog Stewart platform consists of two platforms and six linear actuators connecting through universal joints. The Stewart platform has 6 DOF, which gives the possibility to perform different forms of displacements.

The steering wheel feedback plays an important role to create high reality feel of driving in driving simulator. Chalmers simulator employs a brushless DC servo motor to create a steering wheel feedback torque on the steering wheel. The motor is mounted on the shaft behind steering wheel.

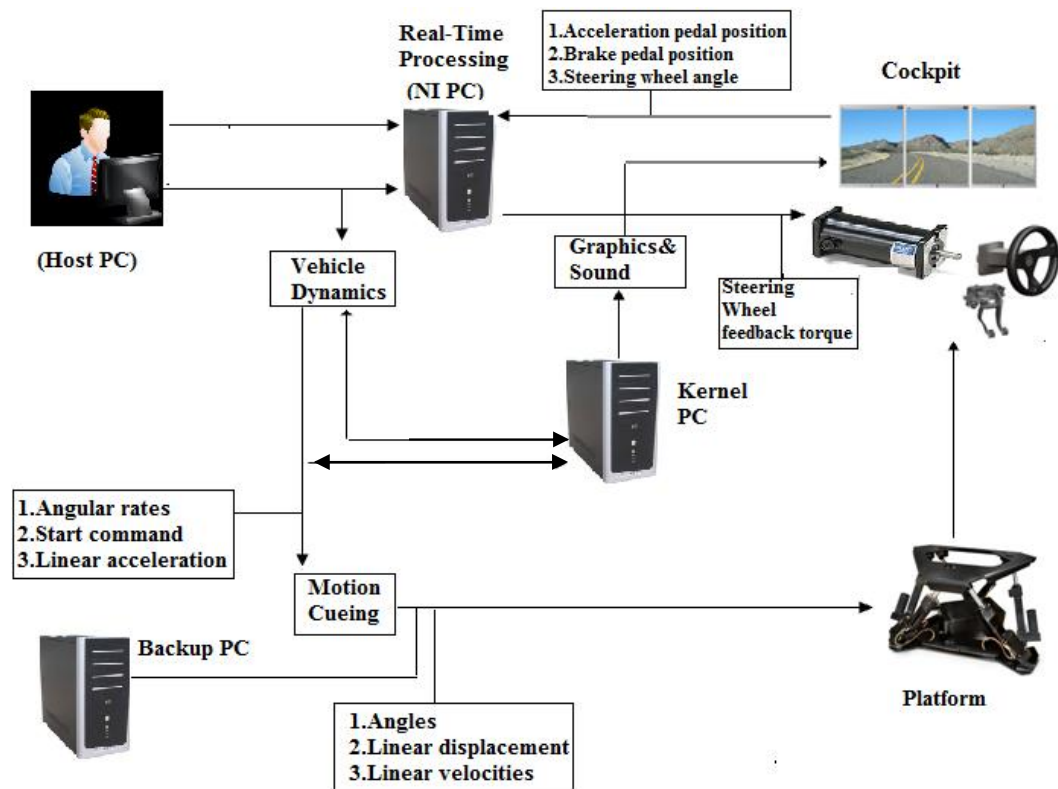


Figure 1.1: Simulator architecture



Figure 1.2: Chalmers S2 driving simulator

1.2 Master thesis's goal

The main goal of this thesis is to develop a new model of the steering system in order to improve the steering wheel force feedback in Chalmers driving simulator. The previous model is developed in Simulink[®], see [2]. The model works well, but the steering geometry model can be improved in Steering system model.

1.3 Model characteristics

The model characteristics must provide the following conditions:

1. It must provide the accurate calculation of the torques on wheels such as: Self aligning torque, frictions torques, stiffness and dampers torques.
2. Parameterization of model plays important role to achieve more realistic steering feel, in order to achieve more realistic model must be parameterized with considering a real vehicle's specifications.
3. It must be designed as simple as possible to modify so that it can be used to represent different cars.
4. The LKAS system is proposed in this thesis such that the desired path is generated to minimize the trajectory overshoot.

1.4 Model limitations

The model is developed to present vehicle behaviour when driving in normal condition of roads and cars, so it can not be reliable in non-linear conditions (When the vehicle is driven up to its limits).

The model developed in this project does not represent the steering condition in parking situations. The model is developed by assuming that the wheels are in contact with the road surface. So the wheel lift phenomenon is assumed negligible in this model.

2. VEHICLE DYNAMICS MODEL

The aim of this section is to describe the vehicle model used in this thesis. As mentioned earlier, the model, [2], is implemented in Matlab®/Simulink®. The model is made out of seven sub-blocks consisting of Steering geometry, vehicle control, power train, brakes, suspensions, chassis and wheels.

The Simulink® model exists in two versions: offline and online. The differences between the two models are in the input and output sources.

Online model or Hardware-in-the-loop mode can be used in Real-Time simulations. The inputs in this mode are real signals that are transmitted from the driver through steering wheel, acceleration pedal and brake pedals to the National Instruments (NI) data acquire system.

Offline model is usually used during the early development phases before connecting to the data acquiring system, when frequent changes are needed to configure the model.

2.1 VDM structure of XC90 Volvo used in this report

The model consists of 7 sub-blocks that model the steering geometry, power train, brakes, wheels, suspension, chassis, vehicle control. The vehicle control block consists of an active safety system used during simulation. Figure 2.1 shows a schematic of the used VDM model in the report.



Figure 2.1: VDM structured in sub-blocks used in this project

The main sub-blocks are:

1. Steering geometry: This block is established to calculate the steering angle of the wheels by using the steering wheel angle as input. Outputs of this block are the wheel angle for front and rear tires of the model in consideration of steering system forces and road condition.
2. Power train: The main goal of this block is calculation of the engine speed and engine torque required in this model. In order to simulated the power train of the simulated vehicle, The model is supplied with a 2,5 liter engine and the corresponding automatic transmission system from Volvo cars.
3. Brakes: This block is used to model the actual braking torque applied to the brakes for each wheel of the simulated vehicle. Brakes block contains a simplified modeling of hydraulic brake.
4. Wheels: This block contains 4 subsystems for front and rear tires to calculate the tire forces during steering. All the required information about

the tire forces and self aligning torque is calculated in this block. For this reason this block has an important role in this project. In this item TMEasy tire model is used as a virtual tire model. More details about the model are presented in the tire model item.

5. Suspension: This block computes the load transfers and the individual vertical load generated on each tire. In this model the toe and camber angles for the wheel are constant. The absence of changing in toe and camber angles would have led to a high fidelity model. But no big effects were expected in the result of this project, because this project is focused on the steering system.
6. Chassis: This block is used for calculation of the vehicle velocities, accelerations and corresponding coordinate of the vehicle position in IOS coordinate system and world coordinate system. The outputs of this subsystem are the vehicle accelerations, velocities and positions.
7. Vehicle control: All the safety development modeling of the vehicle are located as sub-systems in this block. The main active safety systems to be developed such as Anti-lock Brake System (ABS), Electronic Stability Control (ESC) And Electrical Power Steering Assisted system (EPSA) are located in this subsystem.

2.2 Coordinate systems

In the following section, the basic concepts of the coordinate systems used in this project will be presented. In this model, the ISO coordinate systems are used. They are based on the seven coordinate systems as following:

- Earth (X, Y, Z)

The global coordinate system describes the entire environment of the model. It is used as the position reference for the vehicle because of the global coordinate system which does not move during simulation.

- Vehicle (x, y, z)

The Center of Gravity (COG) coordinate system describes the position of COG during simulation. In this coordinate system, the x-axis is parallel to the longitudinal movement of the vehicle and points to the front of the vehicle. The y-axis is parallel to the lateral movement of the vehicle and the Z axis is parallel to the vertical movement of the vehicle.

- Wheel (x_w, y_w, z_w)

The wheel coordinate system is located in the center of each wheel. In this coordinate system, the x-axis points to the heading of the wheel.

- Path (x_p, y_p, z_p)

The velocity coordinate system is fixed to the center of gravity of the vehicle. The difference of the center of gravity positions follows the velocity vector of the vehicle such as: longitudinal velocity (in x axis direction), Lateral velocity (in y axis direction), vertical velocity (in z axis direction)

- Yaw (ψ)

Yaw is the rotation around the vertical axis (z-axis) through the center of gravity of the vehicle. The yaw can be felt in skidding or spin movement.

- Pitch (ϕ)

Pitch is the rotation around the lateral axis (y-axis) through the center of gravity of the vehicle. It can be felt in acceleration or braking movement around (y-axis) of vehicle.

- Roll (Θ)

Roll is the rotation around the longitudinal axis (x-axis) through the center of gravity of the vehicle. This rotation can be felt during lateral acceleration (side-to-side movement) of the vehicle.

The overall scheme of ISO coordinate system is shown in Figure 2.2.

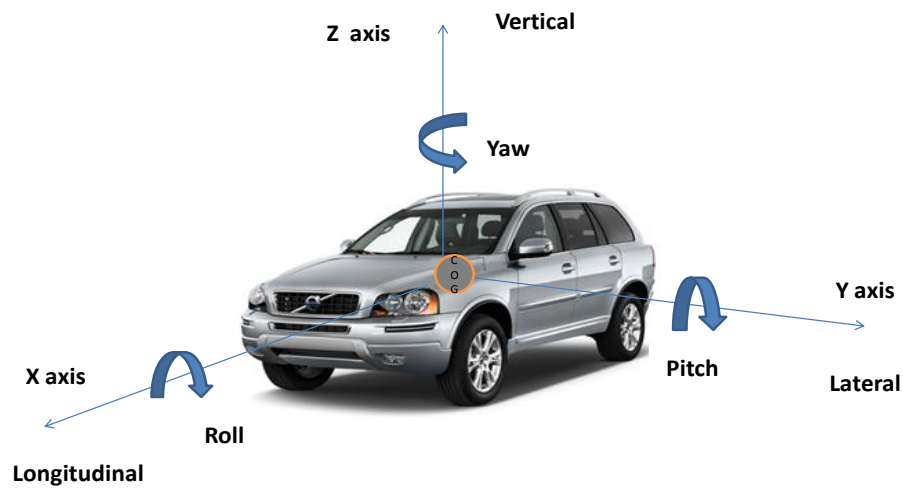


Figure 2.2: Overall scheme of ISO coordinate system for vehicle

2.3 Model inputs and outputs

Identification of the inputs and outputs for the Vehicle Dynamics Model (VDM) is one of the basic steps needed to develop the model. The received information from the simulator platform and Kernel PC, to the VDM is known as model input. The information generated by the VDM and sent to the simulator system is known as model output.

The VDM inputs related to driver behavior that are acquired by National Instruments Digital /Analog and Analog / Digital boards, are listed in Table 2.1.

In order to run an experiment on a driving simulator, it is necessary to have some calculated information from VDM such as vehicle velocities, steering wheel torque, vehicle acceleration. The model developed to calculate the different requirements of the special experiments as VDM outputs.

Table 2.1: VDM inputs

Input	Description
Steering wheel angle	Steering wheel position. Values between [-360, 360], [degree]. Negative for left turn
Acceleration pedal position	Accelerator pedal position. Values between [0, 1] being 1 for full acceleration
Brake pedal position	Brake pedal position. Values between [0, 1] being 1 for full brake.

Table 2.2 shows the some required outputs in related to this project.

Table 2.2: VDM outputs

Output	Description
Vehicle velocities	3 components of the vehicle velocity in IOS coordinate system (Longitudinal, Lateral, Vertical), measured in SI units, [m/s]
Steering wheel torque	Force feedback torque to be generated on steering wheel, measured in SI units, [Nm]
Vehicle Accelarations	3 components of the vehicle acceleration in IOS coordinate system (Longitudinal, Lateral, Vertical) rate, measured in SI units, [m/s ²]
Vehicle slip angle	Difference between the travelling direction of vehicle and the direction that the body of vehicle is pointing. measured in SI units, [rad]
Vehicle angular velocities	3 components of the vehicle angular velocity in IOS coordinate system (Yaw, Roll, Pitch), measured in SI units, [rad/s]
Vehicle angular accelerations	3 components of the vehicle angular acceleration in IOS coordinate system (Yaw, Roll, Pitch) rate, measured in SI units, [rad/s ²]
Offset from middle road	Distance between the COG and middle of road, measured in SI units [m]

The outputs of VDM are sent to the Kernel PC in order to control the simulator platform motion and graphic controlling. The information contains 3 components of vehicle velocities and accelerations, which are used to control the motion platform. Steering wheel torque is generated by a dc servo motor mounted on the steering shaft.

2.4 Model terminology

In this part, vehicle dynamics terminology used in this project is shown in Figure 2.3 and descrined respectively.

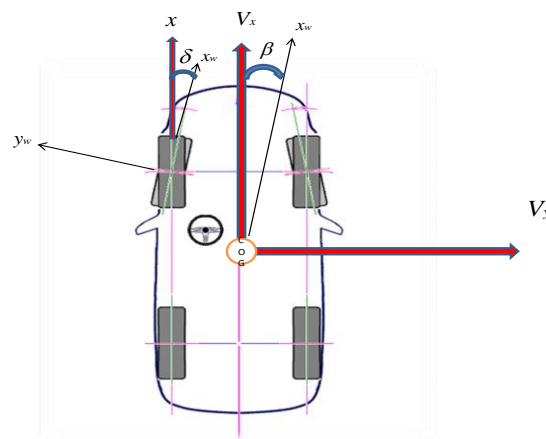


Figure 2.3: Vehicle dynamics terminology used in this project

- Wheel angle (δ)

The Wheel angle (δ) is the angle between the longitudinal axis of the wheel (x_w) and the longitudinal axis of the center of gravity (x) of the vehicle.

- Self aligning torque (M_z)

Self aligning torque (SAT) is a torque created by tire when it is rotated around its vertical axis. Self aligning torque is one of the important parts of the steering wheel force feedback that the driver can sense on the steering wheel. In order to create a high fidelity of steering feel on a driving simulator, the tires modeling need to be developed accurately.

- Side slip angle (β)

The side slip angle(β) is the angle between the longitudinal axis of the path coordinate system (x_p) and the longitudinal axis of the center of gravity (x) of the vehicle.

The side slip angle shows sliding rate of the vehicle, and plays an important role in vehicle safety studying.

- Under steering

The under steering is what occurs when the car does not turn enough to stay on the road. In other words under steering is what happens when the vehicle's side slip angle is less than the steering angle intended by the driver.

- Over steering

The over steering is what occurs when the car turns more sharply than intended by the driver which can get it into a spin. In over steering terms the vehicle side slips angle is more than the amount commanded by the driver.

2.5 Tire modelling

Tire modeling plays an important role in vehicle dynamics modeling. Calculation of tires forces is important to create a high reality steering feel for the driver. Tires are the only part of a vehicle which have contact with the road, so the generated forces between tires and road have an effect on the vehicle motion. On the other hand, tire modeling provides useful information about the road condition by the steering wheel force feedback through the steering wheel. Regarding to this fact that the knowledge of tire forces and individually self aligning torque are essential and valuable for steering systems modeling, the tire modeling should be carefully validated.

The information of direction, magnitude and limit of the forces generated inside the contact path between the tires and road are valuable to compute the self aligning torque for each tire. Self aligning torque also known as aligning moment is the resultant of the tire lateral force and the trail arm of the tire. Self aligning torque attempt to decrease and return the wheel states to zero slip angles.

Tire feedback forces are a combination of two forces:

- Friction (sliding) in the contact path between tire and road surface.

- Elastic deformations (slipping) of the tires due to the longitudinal, lateral and vertical forces on tires.

In recent years, a large amount of research has been done in order to investigate the tires behavior during driving. The classification of different tire models is based on different approaches used to develop the models, so tire model should be selected with consideration to the experiments or simulation requirements of the model. It is important to notice that the most accurate model is not necessarily the best option for each simulation.

Tire models are divided into 3 main categories:

- Empirical model: This category is over parameterized and it is not when there are no measurement data available.
- Theoretical model: This category defines a steady-state and transient phenomenon affecting the tire response in great details. This level of detail is used to develop new tires simulation but This model has no effective application for complete vehicle dynamics simulation.
- Semi-empirical model: This category includes the empirical and theoretical characteristics. Semi-empirical models contain measured data and strategies used in theoretical model as well. Computation speed reduction and high accuracy are advantages of this model.

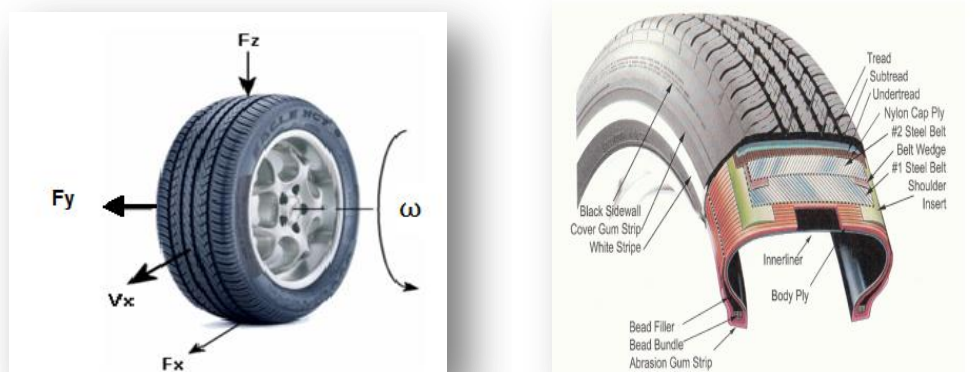


Figure 2.4: Schematics of tire forces adapted from [15]

2.5.1 TMEasy tire model

Considering the importance of tire model in vehicle dynamics modeling and regarding to requirements of this project e.g. lateral and longitudinal forces and self aligning torque, the The TMEasy tire model is based on a semi-empirical approach.

TMEasy tire model was chosen for these reasons:

- This model has ability to accurately simulate the interaction between longitudinal and lateral forces.
- In vertical load changing of vehicle, TMEasy model takes into account the non linear response of the tires as well.
- This model combines the advantages of the mathematical approaches with a experimental parameter set of physical meaning and the model runtime is close to Real-time execution time.
- This model simulates characteristics that are physically comprehensible for the user.
- This model is being used by Volvo cars, so it allows us to access some measurement data for the tires.

2.5.2 Longitudinal forces

The longitudinal forces are generated between tire and road, due to the difference in velocity between road and tire, when accelerating and braking. This difference between the rotational speed of tire (ω) and vehicle longitudinal speed (v) is called longitudinal slip or slip rate (s). The tread elements in the tire will deform when the slip is non zero. This deformation generates a force on the tire that causes the vehicle move. The slip rate is different for acceleration and braking. The slip rate can be calculated as follows:

$$s = \begin{cases} \frac{v - R.\omega}{v} & ,\text{for braking } (R.\omega < v) \\ \frac{R.\omega - v}{R.\omega} & ,\text{for acceleration } (R.\omega > v) \end{cases} \quad (2.1)$$

where ω is the rotational velocity and R is the radius of tire, v is the longitudinal velocity of the vehicle. The value of the longitudinal slip is limited such

that $|S| \leq 1$. For braking, axle speed is used in denominator of equation so that the longitudinal slip is 1 for $\omega=0$ (braking).

Increasing the slip of tire causes increasing of force as well, on the other hand the longitudinal force is generated mostly depending on the construction of tire, the road condition and the vertical force applied on the tire. The main reason of force increasing is that the thread element of tire will be deformed and create the longitudinal force. The slip has linear relation with force for low slip rates, so the slope of this curve is called longitudinal tire stiffness. The longitudinal force decreases because the thread elements become saturated and unable to generate more force and the tire is locked for this condition.[2]

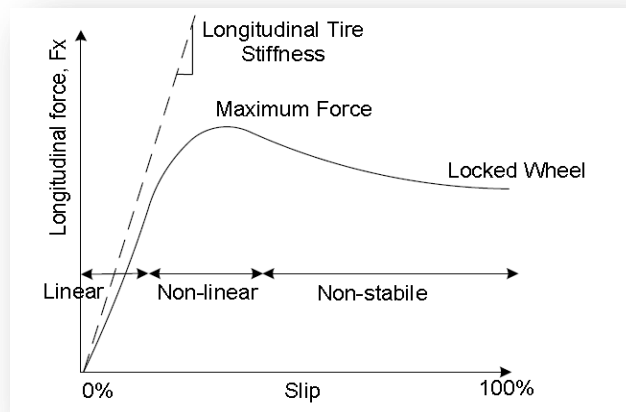


Figure 2.5: Longitudinal forces vs. slip in the tire coordinate system, Adapted from [2].

2.5.3 Lateral force

The lateral force on a tire is proportional to the slip angle of the tire. Generation of lateral force on the tire is similar to longitudinal forces that are described in the previous item. It depends on the magnitude of lateral deformation of the treads in the contact patch. For this reason, the lateral force is proportional to lateral slip angle for small slip angles. Lateral slip is the angle formed by the longitudinal axis (V_x) and lateral axis (V_y) of tire velocity. The overall schematic of tire slip angle is shown in Figure 2.6.

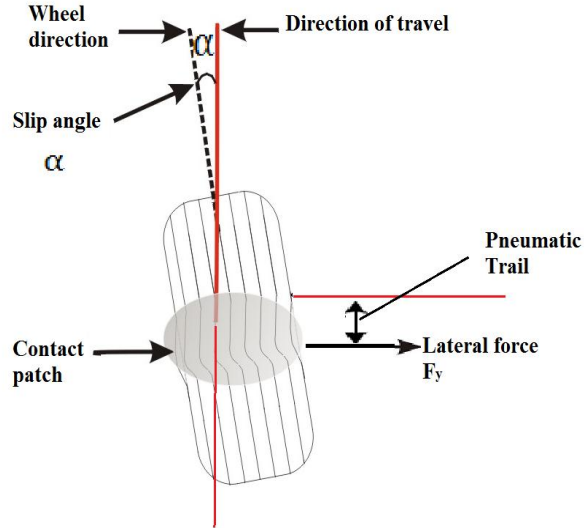


Figure 2.6: Tire slip angle and tire pneumatic trail schematic

The slip angle (α) is calculable as follows:

$$\alpha = \tan^{-1} \frac{V_y}{|V_x|} \quad (2.2)$$

where V_y is the lateral axis of velocity parallel to the direction of travel at the contact path and V_x is the longitudinal axis of velocity (Wheel direction affected by lateral force) on the tire coordinate system.

In order to investigate lateral forces limitation at the tire, we must estimate both front and rear axle lateral forces. The front and rear lateral forces equations are shown as follows:

$$F_{yf} = C_f \cdot \alpha_f, \text{ Front tire lateral force} \quad (2.3)$$

$$F_{yr} = C_r \cdot \alpha_r, \text{ Rear tire lateral force} \quad (2.4)$$

where C_f and C_r are the front and rear tires cornering stiffness respectively, In fact the initial slope of the force vs. slip graph is called the cornering stiffness. The C_f and C_r used for this project are extracted from vehicle constant of XC 90 Volvo.

The α_f and α_r are the front and rear tire slip angles respectively, and can be calculate as follows:

$$\alpha_f = \delta - \tan^{-1}\left(\frac{\dot{y} + \dot{\psi}l_f}{\dot{x}}\right) \quad \text{or} \quad \alpha_f = \delta - \beta - \frac{\dot{\psi}l_f}{v}, \text{Front slip angle,} \quad (2.5)$$

$$\alpha_r = -\tan^{-1}\left(\frac{\dot{y} - \dot{\psi}l_r}{\dot{x}}\right) \quad \text{or} \quad \alpha_r = -\beta + \frac{\dot{\psi}l_r}{v}, \text{Rear slip angle,} \quad (2.6)$$

where δ is the steering angle and β is the side slip angle at the COG that can be calculated by using equation 2.7 is shown in the following. The \dot{y} and \dot{x} are the derivative of lateral and longitudinal displacement respectively. The $\dot{\psi}$ is vehicle yaw rate at the COG.

$$\beta = \sin^{-1} \frac{u}{v} \quad (2.7)$$

where u is the x-axis of longitudinal velocity and v is the COG of the car's velocity.

2.5.4 Self-aligning torque

Self-aligning torque is the torque that the tire creates when the side slip angle is not zero. In fact, the tire develops this torque when it is turning around the vertical axis, this torque intends to steer the tire direction toward the traveling direction of COG. In fact, it should be considered that the lateral forces do not affect exactly at the center of contact patch, rather it acts at the longitudinal distance between the resulting force and hub's vertical projection known as the tire pneumatic trail (t_p). Pneumatic trail is caused by lateral force at the tire along the length of the contact patch creating a torque about the steer axis known as self-aligning torque [2].

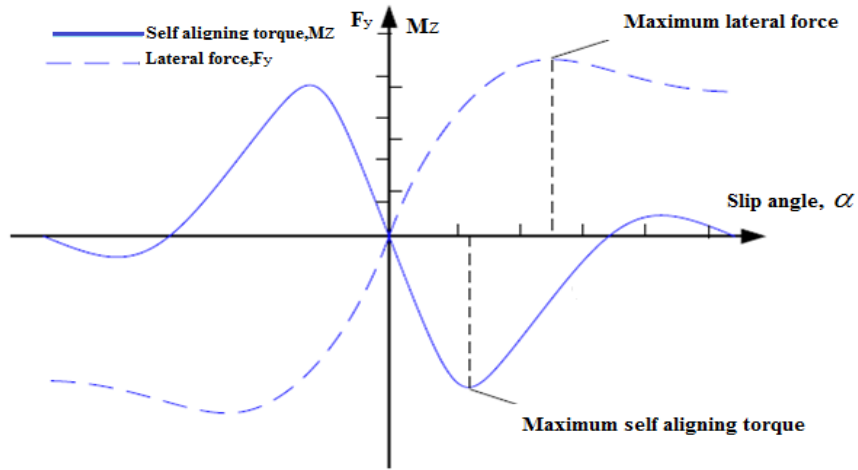


Figure 2.7: Lateral force& self-aligning torque vs. tire slip angle, from [2].

Figure 2.7 shows how self-aligning torque and lateral force depend on the slip angle. The maximum self-aligning torque occurs for a lower slip angle than the maximum lateral force. This means that a decrease in self-aligning torque occurs before the maximum lateral force is reached, see e.g. [2].

As previously mentioned the self-aligning torque can be calculated by product of lateral force and moment arm. The moment arm generated by pneumatic trail (t_p) and the mechanical (caster) trail (t_m). Mechanical trail is a function of steering geometry and can be determined as a function of the steer angle [4]. So, the self-aligning torque can be calculated as follows:

$$M_z = F_y \cdot (t_p + t_m) \quad (2.8)$$

Figure 2.7 shows how the lateral force and self aligning torque are changed with the slip angle, the pneumatic trail will decrease when the self aligning torque decreases to become negative for a very high slip angle. It can be shown the self aligning torque and lateral force decrease when maximum lateral force has been reached, in other words the pneumatic trail has been decreased after maximum lateral force has been reached as well.

2.6 Vehicle model

There are numerous vehicle models to take into consideration for degrees of freedom. A very simple model of the vehicle is a two degree of freedom, bicycle model associated a linear tire model that represents the linear lateral and yaw motions. This model is commonly used for vehicle control studies and it is an easy way to understand the basic concepts of vehicle modeling. An overall schematic of the bicycle model is shown in Figure 2.8.

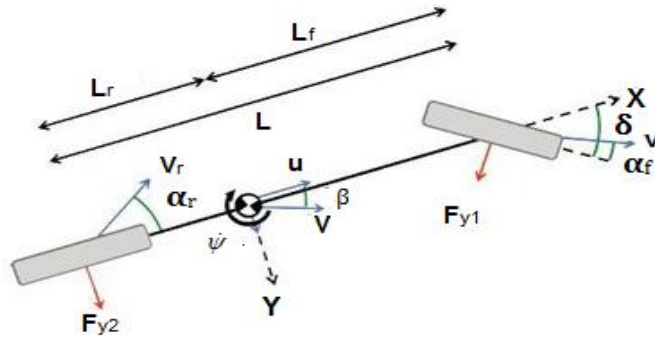


Figure 2.8: Bicycle model schematic

In the following section, the tire forces will be presented. Calculation of the tire forces is the first step of steering modeling in order to study of vehicle behavior. The bicycle model is a linear model and the cornering stiffness is the only parameter used to model the tire.

2.6.1 Equations of motion

As mentioned before, the two DOF bicycle model are mostly used for studying the vehicle motions behavior. The vehicle velocities and acceleration can be calculated by applying Newton's equations for balance of the forces and torques of the complete vehicle.

The equilibrium of torque balance and lateral force balance applying Newton Equations are shown as follows :

$$\sum T = 0, \quad \tau = F_y \cdot l_{\text{arm}} \quad \Rightarrow \quad J_z \cdot \ddot{\psi} = F_{yf} \cdot l_f - F_{yr} \cdot l_r, \quad \text{torque balance} \quad (2.9)$$

$$\sum F_y = m \cdot a_y \quad \Rightarrow \quad F_{yf} + F_{yr} = m \cdot v \cdot (\dot{\psi} + \dot{\beta}) \quad , \quad \text{lateral force balance} \quad (2.10)$$

where F_{yf} and F_{yr} are the lateral forces of front and rear tires respectively:

$$\begin{aligned} F_{yf} &= C_f \cdot \alpha_f, & \text{Front tire lateral forces,} \\ F_{yr} &= C_r \cdot \alpha_r, & \text{Rear tire lateral forces} \end{aligned} \quad (2.11)$$

The equation of slip angles for front and rear tires are described in 2.5.3 and can be calculated from equation 2.2. The 3-D schematic of the chassis forces is shown in Figure 2.9.

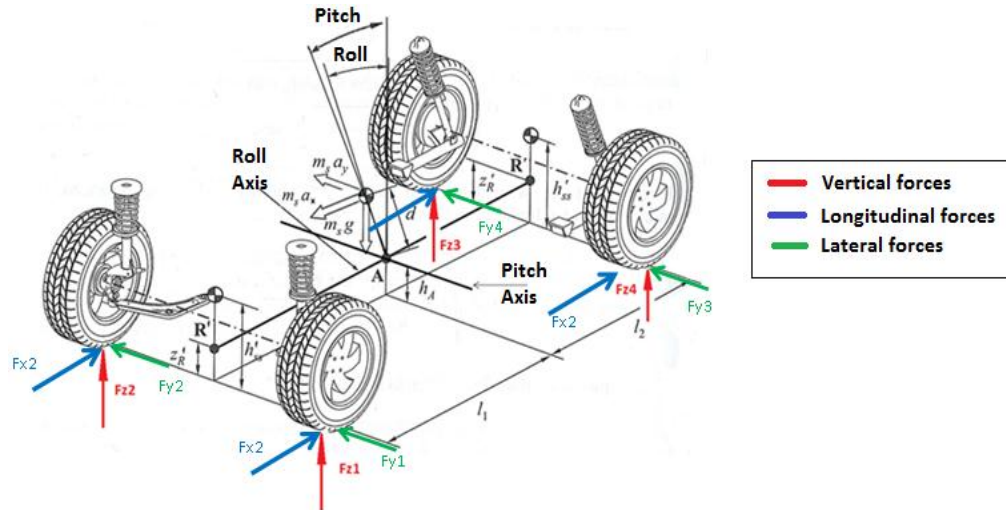


Figure 2.9: Schematic 3D-view of a two-track vehicle, from Luque, Álvarez (2005)

3. STEERING SYSTEM MODELING

In this chapter, the steering system used in this thesis is described. As mentioned before, steering system modeling is one of the most important issues in driving simulation. The high fidelity of steering system simulation is useful to achieve high reality steering feel for the driver during driving simulation.

The steering system modeled during this project consists of two main parts: steering geometry and steering wheel feedback torque. Steering geometry is created to transmit the steering wheel angle applied by the driver as an input to virtual wheels angles as output. Steering wheel feedback torque has the main purpose of transmitting the torque created in a tire (self-aligning torque, friction torque...) to the steering wheel. In other words, steering system model receives the steering wheel position which is applied by the driver as input and provides the steering wheel feedback torque as output.

3.1 Steering system overview

The steering system transfers the steering wheel angle to the wheels through a mechanical system composed by a series of rods and pivots linkages. In this case when the driver turns the steering wheel, the steering wheel's rotation is transmitted through the steering column (steering shaft) to the pinion, the pinion convert the rotation to the linear displacement through the rack and pinion. The created linear movement is transferred to the uprights through the tie rods. The created linear movement at upright generates the steering angle in the wheels. The steering mechanism between the steering box and the steering angle in the wheels presents a transmission rate which is called steering ratio. It is important to notice that the steering wheel angle and wheel angle relates via a steering ratio coefficient.

Rack and pinion steering system is commonly used in conventional cars. In this project, the power steering assistance system is used as well as the rack and pinion system. A power steering assist system helps drivers by decreasing the driver's effort

in the steering wheel. The power steering assistance system is comprised of a DC motor and a control unit, so that the control unit calculates if a steering assistance is required for the driver. More information about the power steering assistance will be presented in the last part of this chapter. The rack and pinion steering system is shown in Figure 3.1 and steering box is shown in Figure 3.2 respectively.

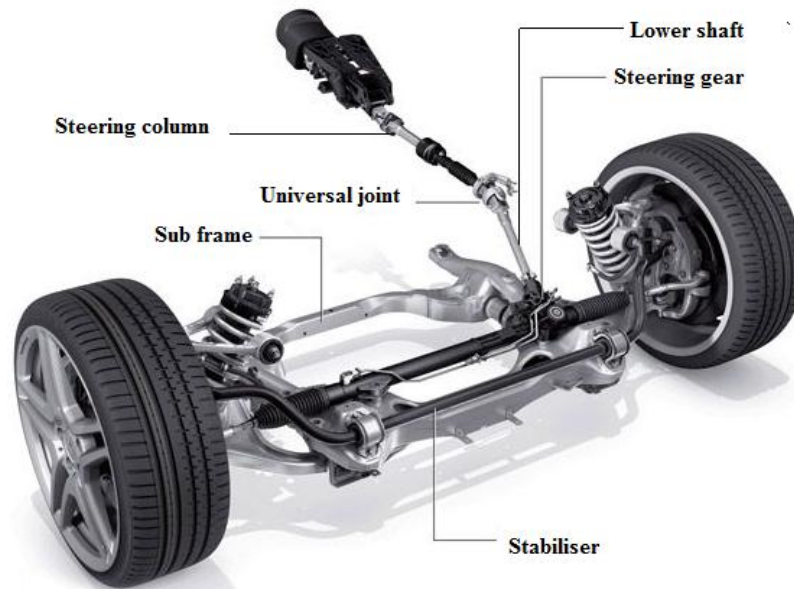


Figure 3.1: Steering systems (rack and pinion).

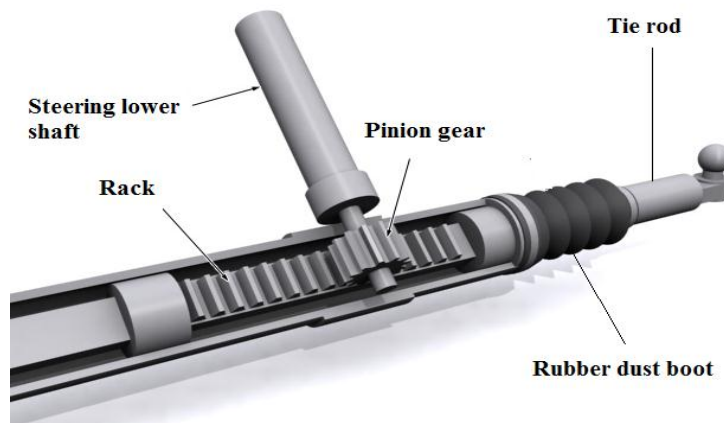


Figure 3.2: Steering gear schematic. Adapted from [16]

In this project the steering ratio of XC 90 Volvo is used to calculate the wheel angles. The mechanical linkage between the steering box and the wheels usually conform to an Ackermann steering system.

Ackerman steering geometry is the term used to describe the behavior of the front wheel when the vehicle is driven around a corner. In the corner when the front tires turn, the inner wheels radius is smaller than the outer wheels and that means the steering wheel is needed to generate the wheel angle for the inner wheels which are larger than the outer wheels, otherwise the inner wheel tends to slide over the road [3]. The Ackerman geometry neglects the effect of road on tire, so it is not completely suitable for modern cars. The wheels behavior interface corner turning can be seen in Figure 3.3.

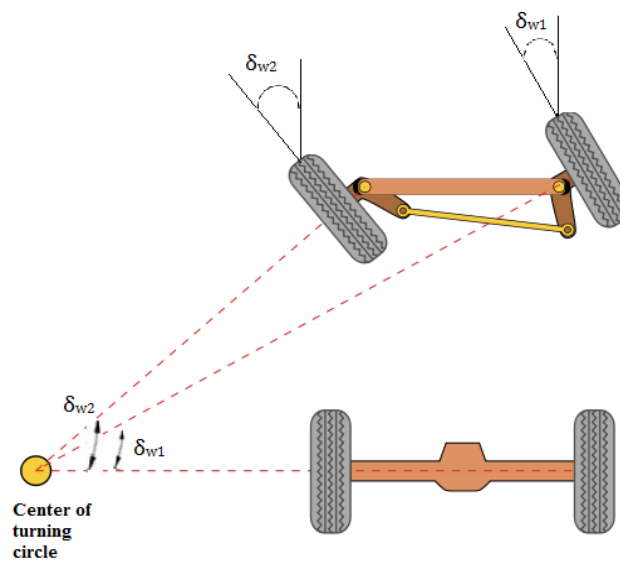


Figure 3.3: Ackerman steering geometry

As can be seen in the Figure, the inner wheel angle is larger than the outer wheel, when the vehicle turns around a circle.

$$\delta_{w2} > \delta_{w1}$$

It is important to notice that the wheels behavior analysis is a very important point to accurately simulate tire forces. For this reason, all the parameters which can affect the tires must take into account in tire modeling. The static toe angles for tires are other main characteristics of tires which should be considered in the modeling of the tire. Toe angle is the initial symmetric steering angle that each tire makes with the longitudinal axis of the vehicle, even when the steering wheel is not turned. The steerable wheels are set to have the toe angles as a function of the static steering geometry and kinematic effects of steering system and tires. Regarding the application

of the steering system, the toe angle can be positive or negative. It can be measured as an angular deflection of the tire at the front of the tire.

Toe-in or **positive toe** is the angle between the centerline of the tire and vehicle when the tires are pointing in towards the centerline of the vehicle. Toe in can be useful in order to improve the vehicle stability of the road car for straight driving and vehicle response in a turn.

Toe-out or **negative toe** is the angle between the centerline of the tire and vehicle when the tires are pointing away from the centerline of the vehicle. Toe out is used for racing cars only, because it can increase the vehicles stability in turning position but it is unstable for straight driving. Toe- in and toe -out of the front tires are shown in Figure 3.4.



Figure 3.4: Toe-in and Toe- out for front tire, adapted from [17]

Other properties that should be considered when modeling a steering system are the effect of caster angle, camber angle and kingpin inclination. Caster angle is the angular displacement of the steering axis from vertical axis in the longitudinal plane (in the side view of tire). The positive caster angle is achieved when the steering axis is inclined toward the rear tires of the vehicle (in the side view) and the negative caster angle is achieved when the steering axis is inclined to the front side of the vehicle.

Caster angle affect the steering feel by creating a self-centering torque to reduce the toughness of steering. For example when the caster angle is positive and the wheel is steered, the lateral forces will create a torque around the steering axis and will increase the self-aligning torque of the tire. Increasing of self-aligning torque causes the steering wheel to align quickly. Furthermore positive caster improves the stability

of vehicle in a turn and reduces under-steering situation of the vehicle when the vehicle is exiting from a turn. Positive caster angle will increase handling of the vehicle when the vehicle is turning but it causes the steering wheel to be tougher to move.

When the caster angle is negative the lateral forces will produce a torque that helps steering. Consequently, the entry of the turn is improved as well as the directionality in low-speed turns, but more over-steering will be presented while exiting from a turn. The advantage is that the steering wheel will be less tough to move, and the disadvantage is that the steering wheel becomes more unstable at a high speed. The value of the caster trail is a compromise between these two exigencies [7]. The professional drivers adjust caster angle in order to improve their vehicle handling stability. The positive and negative caster angles are shown in Figure 3.5.

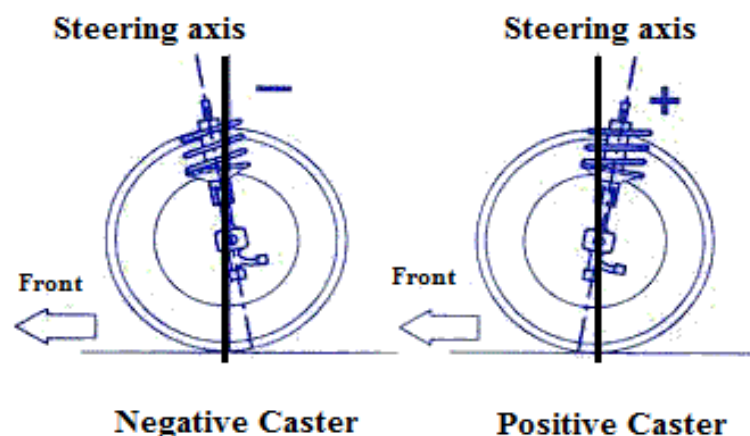


Figure 3.5: Negative and positive caster angles at the top in the side view

The camber angle is the angle made by the wheel between the vertical axis of the wheel and the vertical axis of the steering axis at the top of the front or rear view. Positive caster angle is achieved when the top of the wheel is leaning outward farther than the bottom (at the front view of tire), and if the top of the tire is leaning inward toward the centerline of the vehicle, the negative caster angle is achieved (at the front view of tire). It is important to notice that the cornering force of the tires mostly dependent on their angle relative to the road surface condition, so that the generated

maximum cornering force is achieved at a small negative camber angle. The positive and negative camber angles at the front view are shown in Figure 3.6.

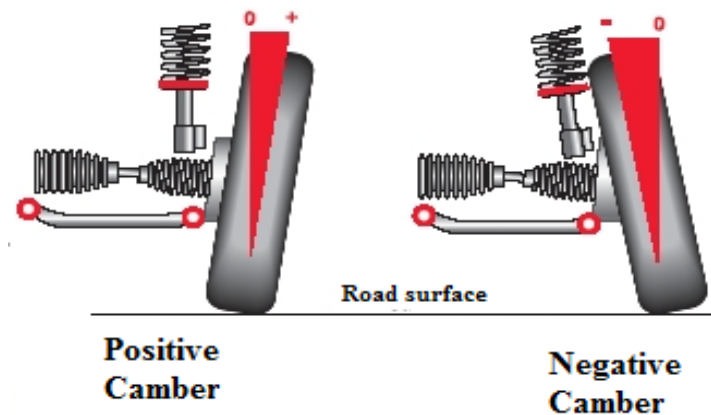


Figure 3.6: Positive and negative camber angles at the front view of the vehicle. Adapted from [18]

Kingpin angle (inclination) is the angle between the kingpin axis and the vertical axis of the tire. The kingpin axis is the line between the lower and upper ball joints of the wheel's hub. The kingpin angle affects the scrub radius at the contact patch of the wheel. The scrub radius is the distance, in range of some millimeters, between the kingpin axis and the tire's contact point with the road, where the kingpin axis and contact patch theoretically touch the road surface.

Positive scrub radius is achieved when the contact point of the kingpin axis with the road surface is internal to the tire's centerline axis (with respect to the frame), this situation is shown in Figure 3.7. The negative scrub radius is achieved when the contact point of the kingpin axis with the road surface is external to the tire's centerline axis (with respect to the frame).

The effect of the kingpin angle is usually discussed in terms of the scrub radius offset which determines the value of the self-aligning torque when the wheels are turned. For the zero scrub radius, no reaction will transmit to the steering wheel and the driver is not able to perceive the change of the vehicle lateral offset. In case of the positive scrub radius (many conventional cars have a positive scrub radius offset) the wheels are returned to the straight position quickly.

In case of the negative scrub radius (some modern cars have a negative scrub radius offset) the longitudinal forces will generate a torque that increases the steering of the

wheels in a longitudinal direction. For this reason, the vehicle becomes more oversteering when the scrub radius offset is negative, thus the driver is not able to sense the self-aligning torque effect correctly. The used scrub radius for this project is extracted from XC 90 Volvo measurement data.

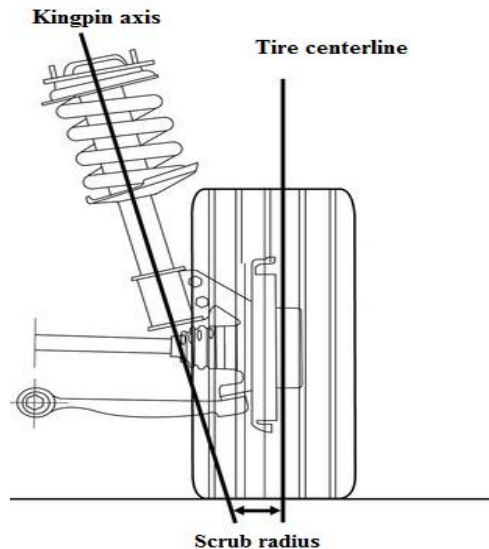


Figure 3.7: Kingpin inclination with the positive scrub radius

3.2 Mathematical modelling of steering system

In this section the mathematical modeling of the steering system used in this project is considered. The steering system is divided into the following two sub-systems:

- The steering geometry block which helps to compute the steering angles measured for each wheel from steering wheel angles as an input. In this part the Ackerman steering system is used, and additionally the effect of the rear toe-in angle has been added to the model in order to improve the stability of the vehicle. The steering geometry used in this project is explained in appendix A.
- The torque feedback block which helps to calculate the steering wheel feedback torque due to the created forces and torques in the tires and steering system (rack and pinion). In this block the mathematical modeling of the

steering system is used. In order to achieve a steering feel as close as possible to real steering, the torque that the driver feels in the steering wheel is important. The steering wheel feedback torque is a result of the tire forces and the steering geometry which is filtered through the power steering sub-system.

3.2.1 Steering system forces and moments

In the modeling of the steering wheel feedback torque, six sources of forces and torques were taken into consideration, they are described as follows:

- Longitudinal forces (F_{Long}): These forces create a torque in the tire when the vehicle accelerates or brakes. The created torque in the tire due to a longitudinal forces is the product of the longitudinal forces and the moment arm. The moment arm in this case is the scrub radius caused by the longitudinal forces effect, which would be sensed in the steering wheel. In this project, the scrub radius is set to a very small value in order to avoid interacting with the braking forces effect when the ESP (Electronic Stability Control) is active. The torque due to the longitudinal forces can be calculated from :

$$\tau_{Whl - Long} = F_{Whl - Long} \cdot \text{scrub radius} \quad (3.1)$$

- Lateral forces (F_{Lat}): These forces create a torque at the contact patch of the tire with the ground. The distance caused by the lateral forces acts as a lever arm and is the sum of the static offset and pneumatic trail which is explained in the 2.5.5. The torque due to the lateral force is the product of the lateral forces and the static offset. This torque is calculated in the *Vehicle/wheels/self-Align-Torque torque* sub-block. The torque due to the lateral forces can be computed as follows:

$$\tau_{Whl - Lat} = F_{Whl - Lat} \cdot L_{Wheel \text{ offset}} \quad (3.2)$$

- Linear damping (b): linear damping of the steering column damper (bs) and the rack (br) generates an opposing torque with respect to the steering wheel rotation direction. The torque due to the linear damping is a product of the damping and the rational speed of the steering wheel.

$$\tau_{damp} = (b_s + b_r) \cdot \dot{\theta}_{sw} \quad (3.3)$$

- Inertial effects: inertial effects of the steering system component such as the steering column, the rack-pinion mass, the wheel carriers and the hubs increase the resisting torque in accelerating and braking. The torque created by the inertial effects is specially noticeable in the rapid reaction of the driver (evasion maneuvers or over reactions in accidents). The torque due to inertial effects is the product of the steering wheel acceleration ($\ddot{\theta}_{sw}$) and a constant factor for inertia (J_s) from XC 90 Volvo measurement data.

$$\tau_{inertia} = J_s \cdot \ddot{\theta}_{sw} \quad (3.4)$$

- Front lift: suspension compliance of the car generates the additional steering angle in the wheels. In order to achieve the high reliability model of the vehicle steering system for the Chalmers driving simulator this part of the model was developed. In this model, the suspension linkage is used to connect the wheels to the body of the car. As mentioned previously, the front wheels of the cars are lifted or lowered due to the caster and kingpin (KPI) angles. The rack and pinion mechanism is used to calculate the proper suspension compliance effect. The model used by the [2] is developed for this project by adding the effect of the caster and KPI angles, which is added to the XC90 model. The suspension compliance used for this model adapted from the vehicle dynamics which was written as [7].
- Friction: friction is one of the important components of the steering system modeling which should be considered in modeling process. In the model used by Benito& Nilsson a constant friction is applied as a dry friction between the road surface and the steerable wheels. The friction modeling for this project was developed through adding the friction that comes from the rack-pinion contact and bearings of the steering systems. Dahl friction model is used to model the rack-pinion component friction, because it is simple and most useful. The Dahl friction model proposed that the relationship between

frictional force and position would be analogous to a stress-strain curve and hysteresis. Modeling of the stress-strain curve can be extracted as:

$$\dot{F}_f(t) = \sigma \cdot \left[1 - \frac{F_f(t)}{F_c} \cdot \text{sign}(\dot{x}(t))\right]^\lambda \cdot \text{sign}\left(1 - \frac{F_f(t)}{F_c} \cdot \text{sign}(\dot{x}(t))\right) \cdot \dot{x}(t) \quad (3.5)$$

where σ is the stiffness coefficient, $F_f(t)$ is the Dahl friction force, F_c is the coulomb friction force, $\dot{x}(t)$ is the velocity between two surfaces and λ is the shape parameter. More information about the friction modeling in this project can be found in friction modeling 3.3.

3.2.2 Mathematical modelling of tire forces

Mathematical model of the steering wheel should be adopted the forces and moments which described in 3.2.1. The steering system model considered is based on the torques and forces and is presented in Figure 3.8.

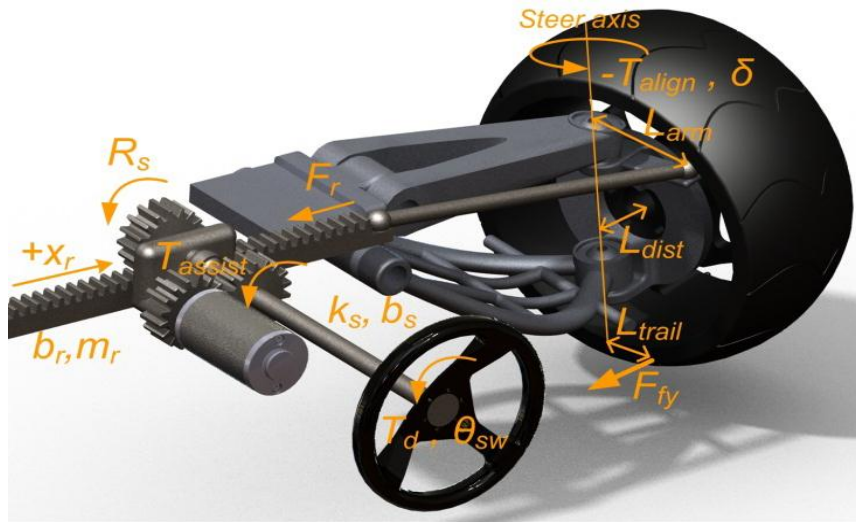


Figure 3.8: Mathematical scheme of steering system. Adapted from [5]

Regarding to the steering system moments, the starting point of the modeling is to calculate the forces in the tires. The longitudinal and lateral forces of the front tires can be calculated by using:

$$\begin{aligned} \sum Fx &= m \cdot ax && \text{,For longitudinal forces} \\ FX &= (F_{xi} - F_{rollingi}) \cdot \cos(\delta_{wi}) - F_{yi} \cdot \sin(\delta_{wi}) && \text{,with } i=1,2 \end{aligned} \quad (3.6)$$

where F_x and F_y are the longitudinal and forces of tire respectively which are derived from TMEasy tire's model (An overall view on TMEasy tire's model can be found in appendix B). The $F_{rolling}$ is the force generated by tire rolling resistance, the $F_{rolling}$ can be calculated from:

$$F_{rolling} = -f_r \cdot m \cdot g \cdot \min(1, V_x) \cdot \text{sign}(V_x) \quad (3.7)$$

where f_r is the rolling resistance coefficient, the m is the vehicle curb mass adding the driver mass (75Kg), g is gravity acceleration and V_x is the longitudinal axis of car's velocity.

The total forces around the steering axle along y direction are:

$$\begin{aligned} \sum F_y &= m \cdot a_y, & \text{For lateral forces} \\ F_Y &= F_{yi} \cdot \cos(\delta_{wi}) + (F_{xi} - F_{rollingi}) \cdot \sin(\delta_{wi}), & \text{with } i=1,2 \end{aligned} \quad (3.8)$$

The total torque generated around the steering axis by FX can be calculated starting from Figure 3.9.

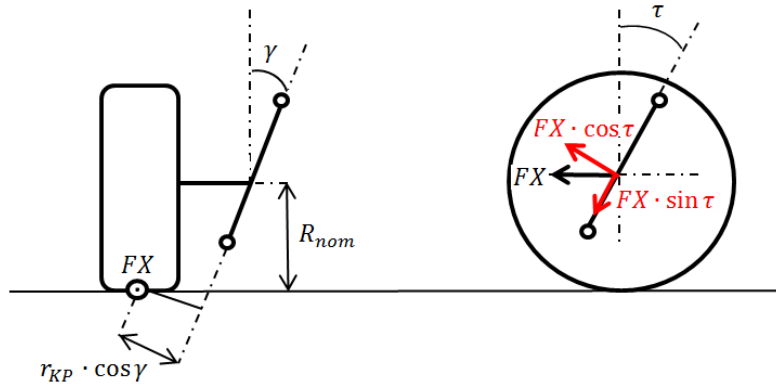


Figure 3.9: Scheme used to calculate the resistant torque generated by FX. Adapted from [7]

As Figure 3.9 shows the total resistant torque generated around the steering axis due to FX can be computed from :

$$\tau_{FX} = FX \cdot \cos(\tau) \cdot [r_{KP} \cdot \cos(\gamma) + R_{nom} \cdot \sin(\gamma)] \quad (3.9)$$

The total resistant torque generated due to FY is calculated by taking into account the effect of the caster and kingpin angles in the contact patch between tire and road surface. The moment arm created due to the caster and KPI is shown in Figure 3.10.

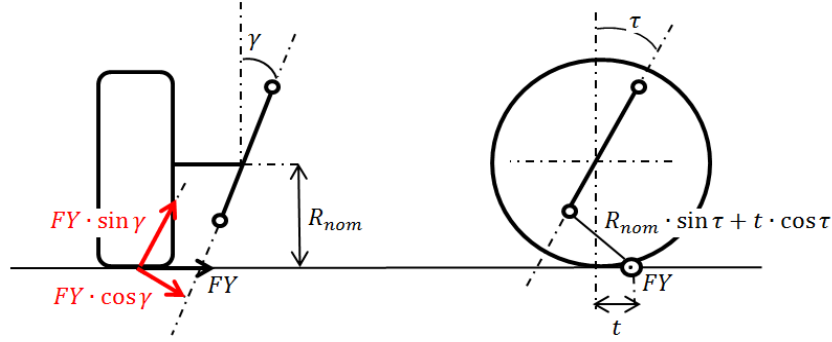


Figure 3.10: Scheme used to calculate the resistant torque generated by FY. Adapted from [7]

Figure 3.10 shows the caster and KPI effect on the lateral forces of tire. So the generated torque due to FY around the steering axis can be determined from:

$$\tau_{FY} = FY \cdot \cos(\gamma) \cdot [t \cdot \cos(\tau) + R_{nom} \cdot \sin(\tau)] \quad (3.10)$$

$$t = t_p + t_m$$

The vertical force and moment generated due to FZ is calculated starting from Figure 3.11.

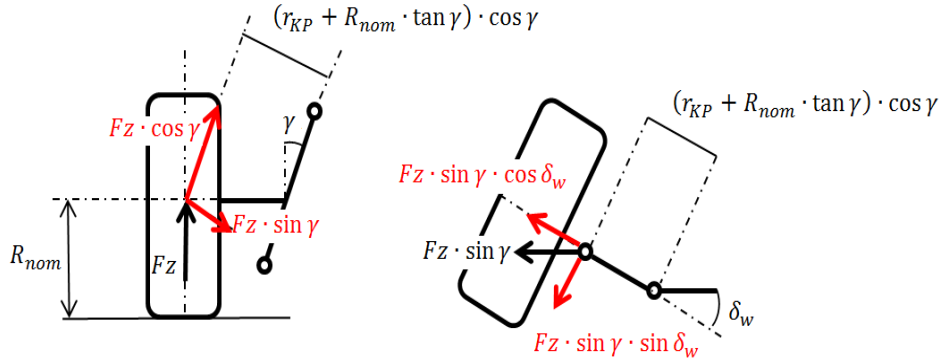


Figure 3.11: Scheme used to calculate the resistant torque generated by FZ. Adapted from [7]

The torque produced due to FZ can be computed from:

$$\tau_{FZ} = F_Z \cdot \sin(\gamma) \cdot \cos(\tau) \cdot \sin(\delta_w) \cdot \{\cos(\gamma) \cdot [r_{KP} + R_{nom} \cdot \tan(\gamma)]\} \quad (3.11)$$

So the total resistant torque generated around the left and right tires of front steering axis can be computed as:

$$\mathcal{T}_{alignW1} = -\mathcal{T}_{FX1} + \mathcal{T}_{FY1} + \mathcal{T}_{FZ1}$$

$$\begin{aligned} \mathcal{T}_{alignW1} = & -FX_1 \cdot \cos(\tau) \cdot [r_{KP} \cdot \cos(\gamma) + R_{nom} \cdot \sin(\gamma)] \\ & + FY_1 \cdot \cos(\gamma) \cdot [t \cdot \cos(\tau) + R_{nom} \cdot \sin(\tau)] \\ & + FZ_1 \cdot \sin(\gamma) \cdot \cos(\tau) \cdot \sin(\delta_w) \cdot \{\cos(\gamma) \cdot [r_{KP} + R_{nom} \cdot \tan(\gamma)]\} \end{aligned} \quad (3.12)$$

$$\mathcal{T}_{alignW2} = -\mathcal{T}_{FX2} + \mathcal{T}_{FY2} + \mathcal{T}_{FZ2}$$

$$\begin{aligned} \mathcal{T}_{alignW2} = & -FX_2 \cdot \cos(\tau) \cdot [r_{KP} \cdot \cos(\gamma) + R_{nom} \cdot \sin(\gamma)] \\ & + FY_2 \cdot \cos(\gamma) \cdot [t \cdot \cos(\tau) + R_{nom} \cdot \sin(\tau)] \\ & + FZ_2 \cdot \sin(\gamma) \cdot \cos(\tau) \cdot \sin(\delta_w) \cdot \{\cos(\gamma) \cdot [r_{KP} + R_{nom} \cdot \tan(\gamma)]\} \end{aligned} \quad (3.13)$$

3.2.3 Mathematical modelling of steering column

In the modeling of the steering column the rack forces should be taking into account. The total torques on the steering axis is mentioned in 3.2.2. The resulting displacement of the rack, x_r , derives from the torque applied by driver and the torques generated by the steering axis and tires on the rack. The rack through the lever arm is connecting to the wheels. The self-aligning torque around the steering axis is transmitted to the rack through the lever arm.

The mathematical modeling of the steering column with these assumptions can be represented in Figure 3.12.

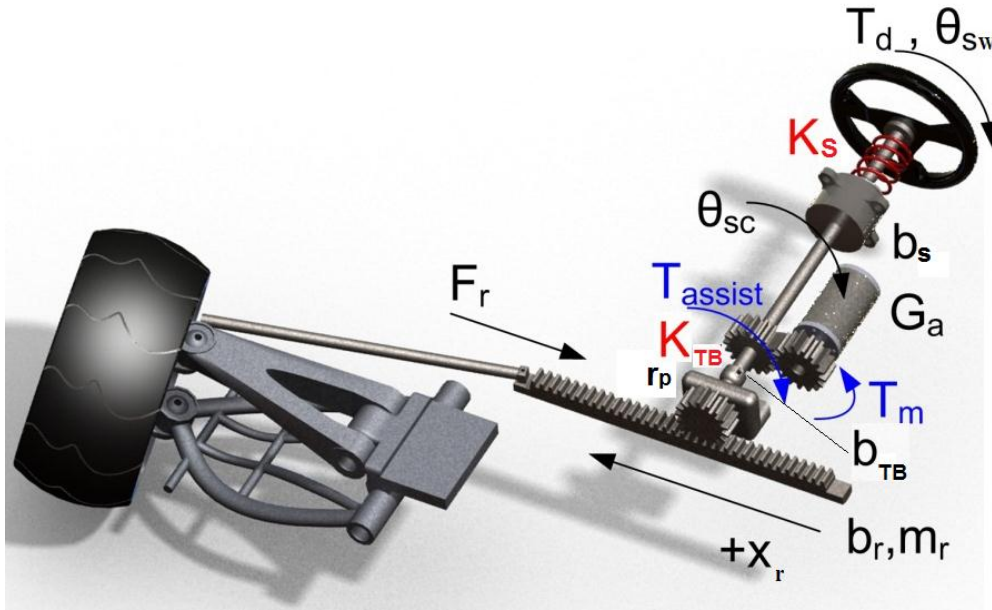


Figure 3.12: Scheme of steering column modelling

The Figure 3.12 shows the steering column torque is composed of the torque applied by the driver (τ_d), the assisting torque generated by the assist motor and the resistant torque generated around the steering axis which is transmitted to the rack through the lever arm. The steering column torque can be computed as:

$$J_s \ddot{\theta}_{SW} = \tau_d + \tau_{assist} - \tau_{TB} - \tau_f \quad (3.14)$$

So to compute the assisting torque and in order to calculate the torque acting on the steering wheel we need to calculate the steering column torque as:

$$\tau_{TB} = k_{TB}(\theta_{SW} - \frac{x_r}{r_p}) - b_{TB}(\dot{\theta}_{SW} - \frac{\dot{x}_r}{r_p}) \quad (3.15)$$

The pinion torque is:

$$\tau_{TB} = F_p \cdot r_p \quad , \text{pinion torque} \quad (3.16)$$

The total force transmitted to the rack can be computed from:

$$F_p = m_r \cdot \ddot{x}_r + b_r \cdot \dot{x}_r + (F_{r1} + F_{r2}) - F_{assist} \quad (3.17)$$

The forces on the rack can be calculated from as:

$$F_{ri} = \frac{\tau_{alignwi}}{L_{arm}} \quad , \text{with } i=1,2 \quad (3.18)$$

And the pinion angle is:

$$\theta_p = \frac{x_r}{r_p} \quad , \text{pinion angle} \quad (3.19)$$

Now that the forces acting on the steering column are known, the torques on steering column can be computed from:

$$\tau_{sw} = J_s \cdot \ddot{\theta}_{sw} + b_s \cdot \dot{\theta}_{sw} + F_p \cdot r_p + \tau_f \quad (3.20)$$

where τ_f is the produced torque due to friction. The detailed view of the friction torque can be found in 3.3.

3.3 Friction torque modelling

As mentioned in 3.2, the friction modeling has an important influence in center-aligning torque of steering axis, so that the friction torque can be affect on tire direction in small steering angle. For this reason the torque is caused by the friction of the rack-pinion contact.

Rotation in different components of torsion bar and dry friction between tire and road surface should be taken into account in steering system modeling.

As described in 3.2 the Dahl friction model was developed for this project. The stress-strain curve is modeled in base of equation 3.21:

$$\dot{F}_f(t) = \sigma \cdot \left[1 - \frac{F_f(t)}{F_c} \cdot \text{sign}(\dot{x}(t)) \right]^\lambda \cdot \text{sign} \left(1 - \frac{F_f(t)}{F_c} \cdot \text{sign}(\dot{x}(t)) \right) \cdot \dot{x}(t) \quad (3.21)$$

where σ is the stiffness coefficient, $F_f(t)$ is the Dahl friction force, F_c is the coulomb friction force, $\dot{x}(t)$ is the velocity between two surfaces and λ is the shape parameter.

The stiffness coefficient for steering wheel can be computed from equation 3.22:

$$\sigma = \frac{2 \cdot b_s \cdot k_s}{\sqrt{\frac{k_s}{J_{sw}}}} \quad (3.22)$$

Dahl friction does not include of the Stribeck effect, In fact the Stribeck effect has a small value and the driver does not perceive it. So the hysteresis in the system should be modeled to compute the friction torque effect. In order to compute the friction torque, the friction forces parameters should be replaced with the friction torques and the velocity between two surfaces should be replaced with the steering wheel velocity. So the friction torque equation can be written as equation 3.23 :

$$\dot{\tau}_f = \sigma \cdot \text{sign}\left(1 - \frac{\tau_f}{\tau_c} \cdot \text{sign}(\dot{\theta}_{sw})\right) \cdot \dot{\theta}_{sw} \quad (3.23)$$

Where the τ_f is the steering wheel friction torque and τ_c is the coulomb friction level and $\dot{\theta}_{sw}$ is the steering wheel angular velocity.

3.4 Power steering modelling

The function of power steering is widely installed in modern cars. The power steering function is used to reduce the effort applied to the steering wheel by the driver, especially when completing a cornering or correction of a car's steering direction at low speed. The power steering systems are categorized in two control methods: Hydraulic Power Assisted Steering (HPAS) and Electric Power Assisted Steering system (EPAS). The power steering system improves the vehicle's safety and helps the driver steering to control a car in unstable maneuvering . In addition the system reduces the driver fatigue during driving, because the power steering system reduces the steering effort of the driver by adding a certain amount of assisting torque to driver's torque (with a relevant amount of the resistant torque through the steering wheel torque). In base of the available measurement data from Volvo, a hydraulic power steering system is modeled in this project.

The basic principle of the HPAS is using an ordinary hydro-mechanical servo parallel to mechanical connection between steering wheel shaft and torsion bar. In HPAS, the steering wheel is connected to the steering rack via the valve which is used to control the amount and direction of the delivered fluid to the cylinder in the steering system closed loop. In this closed loop system, the displacement of the valve and hydraulic adjust the pressure in the cylinder such that appropriate assistance is added to the steering rack [10]. It is important to consider that the driver needs to feel the forces

acting on the steering rack, so the hydraulic system is parallel to steering system. The overall scheme of the hydraulic power steering closed loop is shown in Figure 3.13.

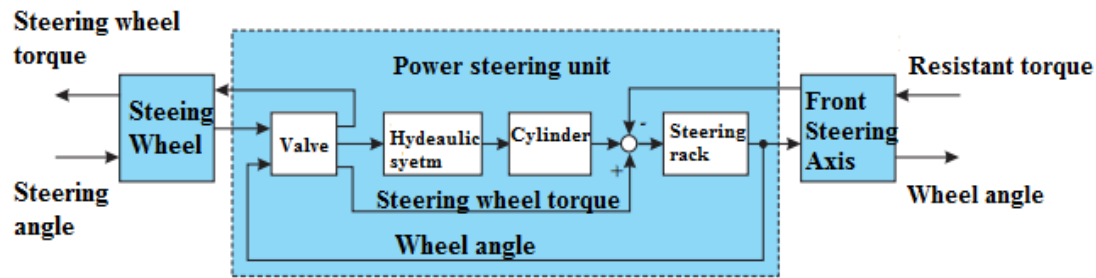


Figure 3.13: Hydraulic power steering closed loop

In the HPAS the fluid is sent to a double acting hydraulic cylinder through the hydraulic system pump, the piston uses the cylinder to produce a force is acting in the steering gear. The structure of the hydraulic power steering system is shown in Figure 3.14.

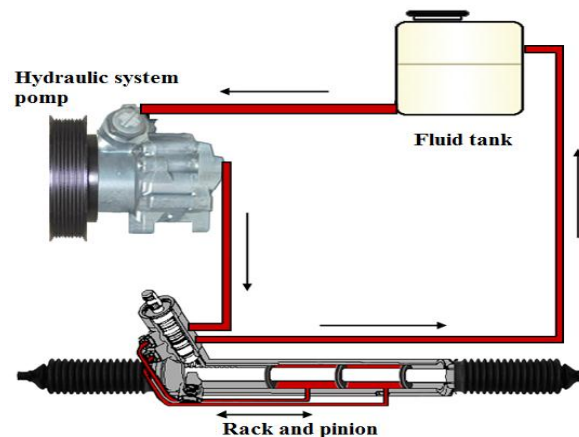


Figure 3.14: Structure of hydraulic power steering system [14]

The attitude of the assisting torque can be determined from the characteristic curve in relation between servo pressure and steering wheel torque. In fact, tuning the assisting torque value is a complicated process because in order to compute an accurate amount of assisting torque we should take into account different factors such as: vehicle types, driving environments, driving styles etc. The amount of the assisting torque would be changed for different condition of driving. For instance when parking, a large amount of assisting torque is needed to make steering wheel as soft as possible, despite the fact that it being not necessary to generate a large amount of assisting torque for

direction corrections or lane changing maneuvers in high speeds. For these reason the typical characteristic between steering wheel torque and boost pressure is shown in Figure 3.15

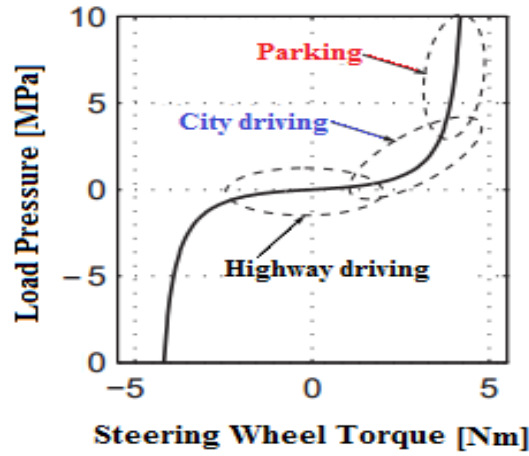


Figure 3.15: Relation between servo pressure and steering wheel torque for different driving condition. Adapted from [10]

The relationship between servo assistance pressure generated by the hydraulic power steering and steering wheel torque can be modeled as:

$$P_{servo-assist} = A \cdot \text{sign}(\tau_{sw}) \cdot (\tau_{sw})^2 \quad (3.24)$$

So the created force by servo can be computed as:

$$M_{servo} = P_{servo-assist} \cdot A_{assist} \cdot r_p \quad (3.25)$$

where A_{assist} is the cylinder working area and r_p is the pinion radius.

The relation between servo pressure and torsion bar torque extracted from XC 90 Volvo is shown in Figure 3.16.

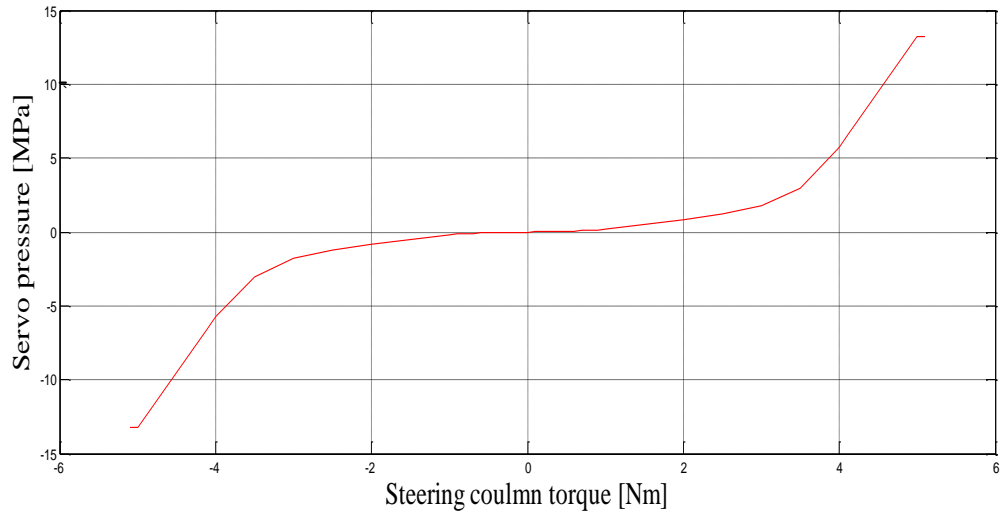


Figure 3.16: Relation between servo pressure and torsion bar torque

The structure of assisting torque function used in this project is shown is Figure 3.17. In this structure the driver's torque is used as an input to power steering boost function from which the resulting assisting torque is computed. The calculated torque is subtracted from the torque that is created by the tires, either by hydraulic circuit [2].

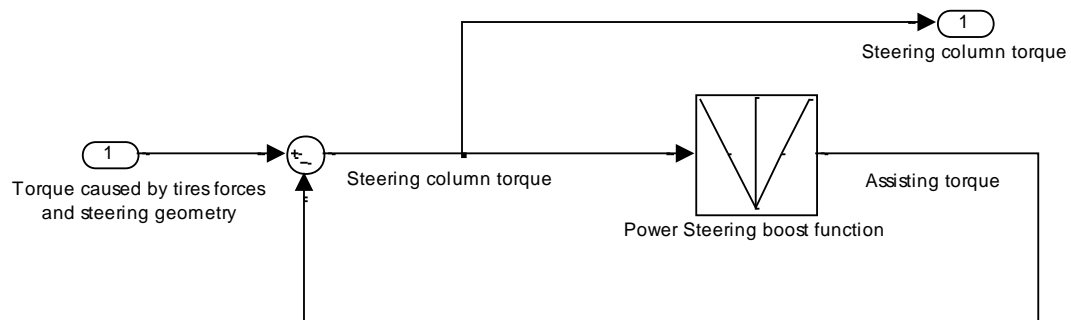


Figure 3.17: Power steering scheme

As Figure 3.17 shows, the steering column torque is input into the system and it is at the same time a direct function of assisting torque output. So this loop requires high computing time. This loop can be able to mange in an off-line simulation, but it is not possible to solve in real-time application [2]. So the layout implemented by [2] is used

for this project. In this simplified layout the torque is caused by the tires forces and steering geometry is used as input for a look-up table, which computes the steering column torque. The driver feels both the steering column torque and the lane-keeping assistance torque in the steering wheel. The implemented layout is shown in Figure 3.18.

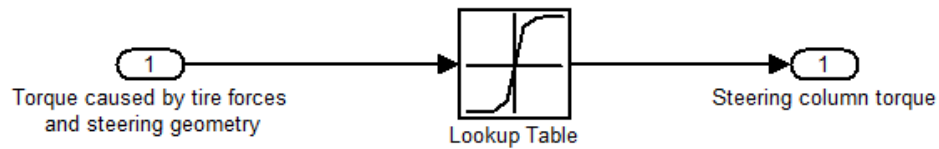


Figure 3.18: Implemented power steering system

More information about power steering can be found in [2],[10]

4. LANE-KEEPING ASSISTANCE SYSTEM

In recent years, improvement to the traffic system safety is widely considered by automotive manufacturers and researchers to reduce the vehicle fatalities. Traffic system safety can be divided into three main factors: human, vehicle and road. The vehicle parameter is investigated in this chapter. Safety of the vehicles can be divided into two areas:

- Passive safety: passive safety provides the safety in structural design of the vehicle in order to reduce the vehicle fatalities when an accident occurs. Passive safety develops the vehicle's chassis and body where no action or intervention by the driver comes into play. Passive safety system intervenes when a crash occurs, for instance airbags and seat-belt tension in the event of a crash.
- Active safety: active safety provides safety of the vehicle stability to avoid accidents. Active safety increases the handling of the car by improving the vehicle stability and driver response. Nowadays, the automotive manufacturers introduce some electronically controlled devices such as : Lane Keeping Assistance(LKA), Hydraulic Power Assisted steering system (HPAS), Electric Power Assisted Steering System(EPAS), Anti-Lock Brake System(ABS), Electronic stability program (ESP).

According to the statistics, more than 50% of vehicle fatalities are the result of unintended lane departure which is caused by the driver's lack of attention. So the lane keeping assistance can be useful to decrease the unintended lane departures as an active safety system. The strategies of LKA can be divided into three parts: development of the functions to determine dangerous situation, design of driver warning system and development of the intervention control strategies to assist driver. The lane keeping system used in this project applies a corrective force to the vehicle based on the lateral offset and heading deviation from the middle lane of the road. In

this system, driver still can intervene by providing a torque in the steering wheel and the driver command is added to the lane keeping assistance command. The lane keeping assistance system analyzed in this project is supposed to keep vehicle in the road in the absence of driver steering command.

Most investigations on the steering wheel force feedback have focused on transmitting the mechanical self-aligning torques which is caused by steering geometry and steering system moments to the driver. In order to to keep the vehicle in the lane, the developed model combines the steering system torque and the lane keeping assistance torque computed by the controller. In this project, a noise is used to warn the driver of an imminent road departure. Some of the warning systems use a warning torque to the driver of imminent lane departure, Sato et al. [11] found that a torque warning to the driver is more effective than sounds while Suzuki [12] found that a torque warning can cause the driver to steer in the wrong direction if not design correctly. [13]

4.1 Lane-keeping controller

The lane keeping controller system is based on the lateral offset and heading distance of vehicle COG. This controller seeks to keep the vehicle between road lanes through the correction of wheel angle by generation a torque in the steering wheel. In this system, the lane keeping assistance torque should be changed when the position of the vehicle changes between lanes. For instance, the system provides zero torque in center lane and increases the torque when the car moves from the specified path. So the lane keeping controller has two parameters: The assistance gain, K_{ass} , which represents the effective torque constant, and a look-ahead distance, X_{la} , which represents the gain of the heading error of vehicle from road's middle lane.

In order to compute a correct value of lane keeping assistance torque, modeling of the vehicle's behavior in unstable condition is necessary. Investigation of the vehicle's behavior before entering a road curve can be useful to study the vehicle's condition before lane keeping occurs. The scheme of the vehicle characteristics before curve is shown in Figure 4.1.

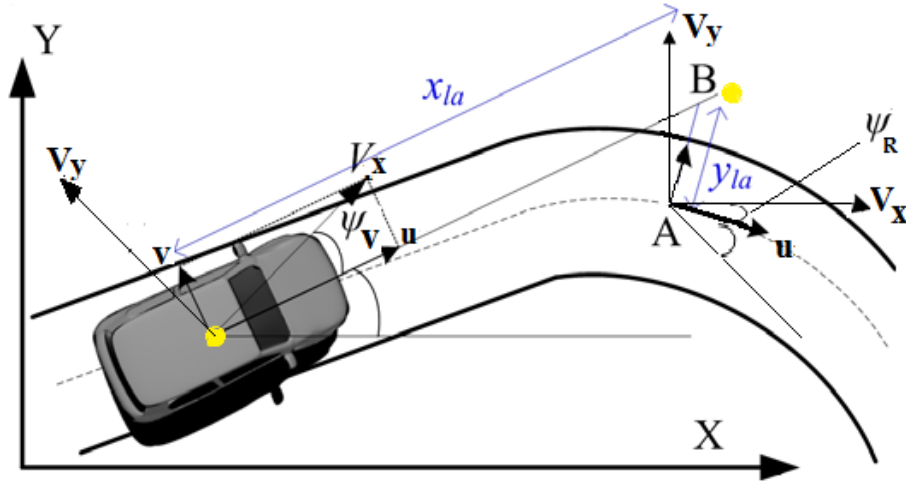


Figure 4.1: Vehicle and road-curve frames.

4.1.1 Vehicle-road model

The modeling of the vehicle-road characteristic is one the important parts of the vehicle's behavior Studying in order to prevent of vehicle road departure. In the following chapter, the characteristic of vehicle velocities is calculated as a function of the yaw angle, longitudinal and lateral forces. It is important to know that this model is suitable for highway traffic so that a slow steering action, slow velocity and small pitch and roll angles are considered. The components of the vehicle velocity in the x-y coordinate read as:

$$\begin{aligned} V_x &= -v \cdot \sin(\psi_v) + u \cdot \cos(\psi_v) \\ V_y &= u \cdot \sin(\psi_v) + v \cdot \cos(\psi_v) \end{aligned} \quad (4.1)$$

where V_y, V_x are the lateral and longitudinal axis of the vehicle velocity before entering to road-curve, and ψ_v is the yaw angle of the vehicle with respect to the centerline before entering to the road-curve.

The time derivative of lateral offset (y_{la}) of the vehicle center with respect to the center-line can be calculated as follows:

$$\dot{y}_{la} = V_x \cdot \sin(\psi_r) + [V_y + (x_{la} \cdot \dot{\psi}_v)] \cdot \cos(\psi_r) \quad (4.2)$$

by substituting equation 4.1 in 4.2 one can obtain:

$$\begin{aligned}\dot{y}_{la} = & [-v \cdot \sin(\psi_v) + u \cdot \cos(\psi_v)] \cdot \sin(\psi_R) \\ & + [u \cdot \sin(\psi_v) + v \cdot \cos(\psi_v) + (x_{la} \cdot \dot{\psi}_v)] \cdot \cos(\psi_R)\end{aligned}\quad (4.3)$$

where ψ_R is the yaw angle of vehicle center in the road-curve. Assuming ψ_v, ψ_R are small enough and R is the road curvature, so that:

$$\begin{aligned}(\sin(\psi_v) \approx \psi_v, \quad \sin(\psi_R) \approx \psi_R, \quad \psi_R \cdot \psi_v \approx 0) \\ (\psi_{vR} = \psi_v + \psi_R, \quad \dot{\psi}_{vR} = \dot{\psi}_v + (-V_x / R))\end{aligned}\quad (4.4)$$

The equation 4.3 can be summarized as:

$$\dot{y}_{la} = v + (u \cdot \psi_{vR}) + x_{la} \cdot \dot{\psi}_v \quad (4.5)$$

The described model can be written in state space as follows:

$$\begin{aligned}\dot{x} &= Ax + Bu + Ew \\ y &= Cx\end{aligned}\quad (4.6)$$

where the state vector $x = [v, r, y_{la}, \psi_{vR}]^T$ contains the vehicle lateral velocity v , the yaw rate r , the lateral offset of COG y_{la} , and relative yaw angle ψ_{vR} . The system's input u , is the front wheel angle and w is the road curvature. A, B, C, D can be computed from 4.7 and 4.8:

$$A = \begin{bmatrix} a_{11} & a_{12} & 0 & 0 \\ a_{21} & a_{22} & 0 & 0 \\ 1 & x_{la} & 0 & u \\ 0 & 1 & 0 & 0 \end{bmatrix}, \quad B = \begin{bmatrix} b_{11} \\ b_{21} \\ 0 \\ 0 \end{bmatrix}, \quad E = \begin{bmatrix} 0 \\ 0 \\ 0 \\ -u \end{bmatrix}, \quad C = \begin{bmatrix} 0 \\ 0 \\ 1 \\ 0 \end{bmatrix} \quad (4.7)$$

$$\begin{aligned}a_{11} &= -(C_f + C_r) / mu, & a_{12} &= (l_f C_f - l_r C_r) / u - mu \\ a_{21} &= -(l_f C_f - l_r C_r) / I_z u, & a_{22} &= -(l_f^2 C_f + l_r^2 C_r) / I_z u \\ b_{11} &= C_f / m, & b_{12} &= l_f C_f / I_z, & u &= \delta, & w &= 1 / R\end{aligned}\quad (4.8)$$

The transfer function from wheel angle δ , to lateral offset y_{la} , as follows:

$$G(s) = \frac{y_a(s)}{\delta(s)} = C(sI - A)^{-1}B = \frac{n_2s^2 + n_1s + n_0}{s^2(d_2s^2 + d_1s + d_0)} \quad (4.9)$$

Where two integrators are due to positional situation of the vehicle and two poles arise from vehicle handling .Equation 4.10 reads the transfer function regarding to XC 90 Volvo:

$$G(s) = 10^2 \frac{1.68s^2 + 10.6s + 5.24}{s^2(0.175s^2 + 1.41s + 2.39)} \quad (4.10)$$

The Bode diagram of the transfer function is shown in Figure 4.2:

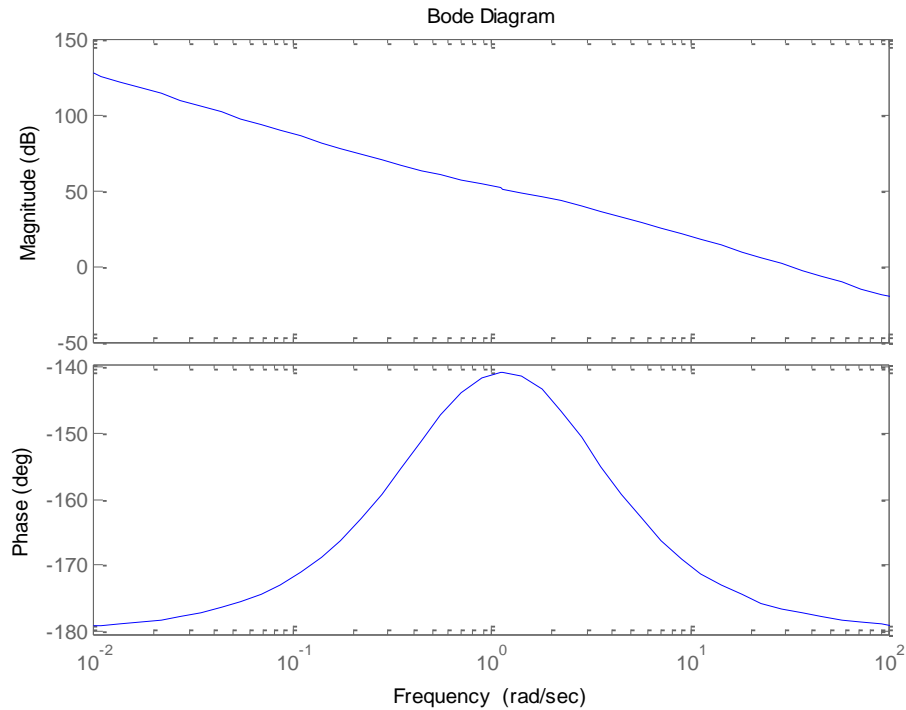


Figure 4.2: Transfer function from wheel angle to lateral offset bode diagram

The nominal parameters used in the model, regarding the XC 90 Volvo data are presented in Table 4.1.

Table 4.1: Nominal value and parameter description

Parameter	Description and range	Nominal value
m	Vehicle mass	2081 [Kg]
C_f	Cornering stiffness of front axle	70000 [N/rad]
C_r	Cornering stiffness of rear axle	140000 [N/rad]
I_z	Vehicle moment of inertia around yaw axis	4512.6 [Kg.m ²]
V_x	Longitudinal velocity of vehicle in range [20-130km/h]	90 [km/h]
L_f	Distance between front axle and COG of vehicle	1.32484 [m]
L_r	Distance between rear axle and COG of vehicle	1.532 [m]
x_{la}	Look-ahead distance of the vehicle' COG in road-curve	25 [m]

4.1.2 Lane-departure prevention controller

As mentioned before, lane-departure is an important factor of serious injuries accidents. According to statistics, more than 1790,000 fatal crashes are recorded relevant to the lane-departure around the world per year. The lane-departure occurs usually by the driver's sleepness, negligence, fatigue and improper reaction of driver in an emergency situation. So the automotive manufacturing such as Nissan, Toyota, Honda have been offering a lane keeping system with audible feedback that sounds if the vehicle begins crossing the lane limit. Since 2002, Toyota and Honda have been offering their lane keeping assist systems that apply steering wheel torque to help drivers to keep the vehicle in the lane [5]. Most lane-departure warning systems utilize a camera to estimate the vehicle position relevant to the roadsides. In this project, a C++ program is used to compute the distance between the centerline of the roads and vehicle COG. The aim of this chapter is to investigate the lane-departure prevention system in emergency maneuver by using the RDP controller developed by Alirezai et al [1]. The controller determines the correcting wheel angle using the steering wheel angle and vehicle's velocity. The overall schematic of RDP controller is shown in Figure 4.3.

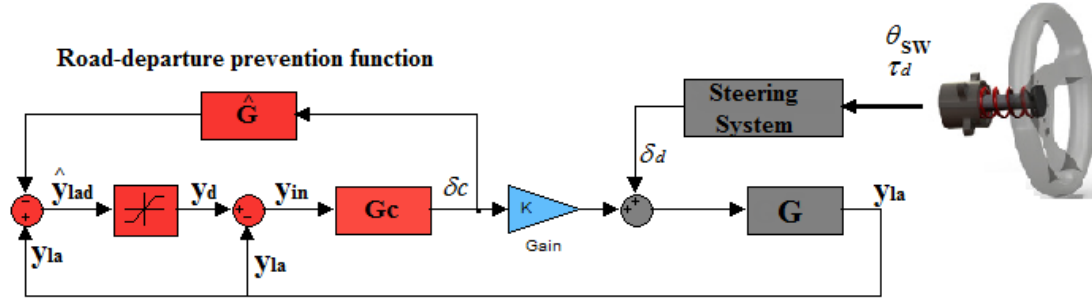


Figure 4.3 : Scheme of road-departure prevention system

In Figure 4.3, block G represents the vehicle dynamics from the front wheel angle δ to lateral offset y_{la} . Block \hat{G} is an estimate of G which was used to account for modeling errors due to correcting angle, \hat{G} function is computed by equation 4.16. The lateral offset y_{la} can be calculated from equation 4.5 and 4.11 as well, where δ_c is the G_c controller's correcting angle and δ_d is the front-wheel steering angle deriving from driver's steering wheel angle θ_{sw} . The estimated desire lateral offset \hat{y}_{lad} is computed as follows.

$$y_{la} = G \cdot \delta \quad \text{when } k=1 \Rightarrow y_{la} = G \cdot (\delta_d + \delta_c) \quad (4.11)$$

$$\hat{y}_{lad} = y_{la} - \hat{G} \cdot \delta_c \quad (4.12)$$

The desired lateral offset y_d can be calculated from equation 4.13, where y_l is the lateral limit (road width). The input of the controller y_{in} is given by equation 4.14.

$$y_d = \eta \hat{y}_{lad} + \lambda \quad (4.13)$$

$$y_d = \begin{cases} -y_l & \text{if } \hat{y}_{lad} < -y_l \\ \hat{y}_{lad} & \text{if } |\hat{y}_{lad}| \leq y_l \\ y_l & \text{if } \hat{y}_{lad} > y_l \end{cases}$$

$$y_{in} = y_d - y_{la} \quad (4.14)$$

Depending on the status of the saturation, the lateral offset function of the wheel angle and road limit can be computed as:

$$\begin{aligned}
\text{if } (\hat{y}_{lad} < -y_l) &\Rightarrow y_{la} = \frac{G}{1+GG_c} \delta_d - \frac{GG_c}{1+GG_c} y_l \\
\text{if } (|\hat{y}_{lad}| \leq y_l) &\Rightarrow y_{la} = y_d \\
\text{if } (\hat{y}_{lad} > y_l) &\Rightarrow y_{la} = \frac{G}{1+GG_c} \delta_d + \frac{GG_c}{1+GG_c} y_l
\end{aligned} \tag{4.15}$$

The order of model's transfer function calculated by 4.9 can be reduced. In order to design a robust controller, Alirezaei et al.[1] the Reduced order transfer function is described as follows:

$$\hat{G}(s) = \frac{m_1 s + m_0}{s^2} \tag{4.16}$$

$$\text{where } m_0 = \frac{1}{l/V_x^2 + K_{ro}}, \quad m_1 = \frac{(x_{la} + l_r)}{V_x} m_0$$

$$l = l_f + l_r \quad \text{and} \quad K_{ro} = m(l_r \cdot C_r - l_f \cdot C_f) / l \cdot C_f \cdot C_r$$

$\hat{G}(s)$ function was used to calculate the desired lateral offset in look-ahead distance. According to the Figure 4.3 when $\delta_c = 0$ and that y_{la} is within the road limits $y_d = y_{la}$, so $y_{in}=0$ and therefore the controller has no effect on the vehicle. When the wheel's angle points the vehicle outside the road limits, so $y_d \neq y_{la}$ and controller input y_{in} is not zero, therefore the controller G_c becomes active ($\delta_c \neq 0$). The Simulink model of vehicle dynamic can compute the look-ahead position and lateral offset of the COG with respect to the road limits. The look-ahead distance in 25 m/s velocity when the time is set to 0.5 is equal to $x_{la}=12.5\text{m}$.

In this section, the correcting wheel angle where is the first point of the required lane-keeping assist torque calculated for controller. The correcting angle can be determined as represented:

$$\delta_c = (k_{ro} V_x^2 + l) \cdot w \cdot \text{steering ratio} + k_{VR} \cdot \psi_{VR} + k_{y_Loff} \cdot y_{la} \tag{4.17}$$

where K_{VR} and K_{y_Loff} are the lane-keeping constant coefficient that they are tuned during the test process, y_{la} is the lateral error between vehicle COG and middle lane of

road. Ψ is the heading error of the vehicle and middle lane of the road and w is the road curvature.

The force feedback based on the lane keeping assistance is proportional to the corrective wheel angle, so the torque caused by the correcting wheel angle can be calculated as shown:

$$\tau_{lka} = K_c \cdot \delta_c \cdot \text{steering ratio} \quad (4.18)$$

where τ_{lka} is an advisory steering torque for lane-keeping which is product of correcting wheel angle δ_c (resulting from controller function G_c). The Steering ratio is the ratio between steering wheel angle and wheel angle $\frac{\theta_{sw}}{\delta_w}$. This ratio is obtained from XC 90 Volvo measurement data(15.9/1). In emergency maneuver, the correcting Wheel angle can be increased quickly, to avoid a high magnitude impulse torque on the Steering wheel. Therefore, τ_{lka} was designed to be limited, where $K_c = 0.5$ Nm/rad)

4.2 Modelling of force feedback generation for lane-keeping assistance torque

The system can be modeled as a mass damper system and implemented as a torque input from the motor. So the model can be described as inertia of the steering wheel and motor. The system can be expressed by:

$$J_s \ddot{\theta}_{sw} + b_s \dot{\theta}_s = \tau_{sw} - \tau_{motor} \quad (4.19)$$

where τ_{sw} is zero if the driver's hands are off the steering wheel. τ_{motor} Contains various force feedback components represented as follow:

$$\tau_{motor} = \tau_{lka} + \tau_{assist} - (\tau_{align} + \tau_{inertia} + \tau_{damper} + \tau_f) \quad (4.20)$$

τ_{lka} is the advisory lane keeping assistance torque which is described in 4.1.2.

τ_{assist} is the power assist torque designed as a function of a driver torque .

τ_{align} is the self-aligning torque caused by the tire forces, the self align torque can be calculated from 3.2.2 equation.

$\tau_{inertia}$ is the torque due to moving parts such as steering wheel and rack inertia which can be calculated as follow:

$$\tau_{inertia} = J_s \cdot \ddot{\theta}_{sw} \cdot \frac{1}{0.05s+1} \quad \text{or} \quad \tau_{inertia} = J_s \cdot \delta \frac{2\pi}{r_p} \cdot \frac{1}{0.05s+1} \quad (4.21)$$

τ_{damper} is the torque due to the artificial damping which is purely a function of the steering wheel velocity:

$$\tau_{damper} = b_s \cdot \dot{\theta}_{sw} \cdot \frac{1}{0.05s+1} \quad \text{or} \quad \tau_{damper} = b_s \cdot \delta \frac{2\pi}{r_p} \cdot \frac{1}{0.05s+1} \quad (4.22)$$

τ_f is the friction torque described in 3.3.

Thus, τ_{motor} can be imposed to the velocity-controlled force feedback motor to create feedback torque on steering wheel. The more details regarding to implementation of force feedback torque via velocity-controlled motor is described in chapter 5.

5. STEERING WHEEL FORCE FEEDBACK IMPLEMENTATION ON DRIVING SIMULATOR

The main goal of the following section is design and implementation of a force feedback steering wheel on driving simulator. In recent years, driving simulator is widely considered within the automotive manufacturing to increase the safety of vehicle in emergency situations. Driving simulations is preferred to real cars of experiments in unstable condition, because it provides safety, repeatability experiments, various parameterizations of vehicle dynamics for vehicle and the environment conditions.

The validity of the acquired measurement data depends on the reality of the simulator. Therefore, improving the driving simulators reality is considered by researcher to increase the driving feel of driver in experiments. Driving simulator reality is usually described by the quality of its motion cueing and visual components. So the control properties and hardware function of the simulator must be taking into account to increase the reliability of the experiments. In this section the schematic of the hardware, control properties and the method to overcome the electromagnetic interfaces are described.

In this study closed loop control method was considered to compute the steering wheel feedback torque. As mentioned in chapter 3 the real car steering system is supposed to compute the forces and moments on the steering system (rack and pinion) for real car. After that, the created torque caused by tires and steering axis is calculated in 3.2. In chapter 4, the lane-keeping assistance torque was calculated to prevent the road departure. According to the publication from Switkes et al.[13] the lane-keeping assistance was calculated in 4.2. The calculated torque is implemented via a brushed DC motor which is mounted on the steering shaft.

The overall schematic of the force feedback system is shown in Figure 5.1.

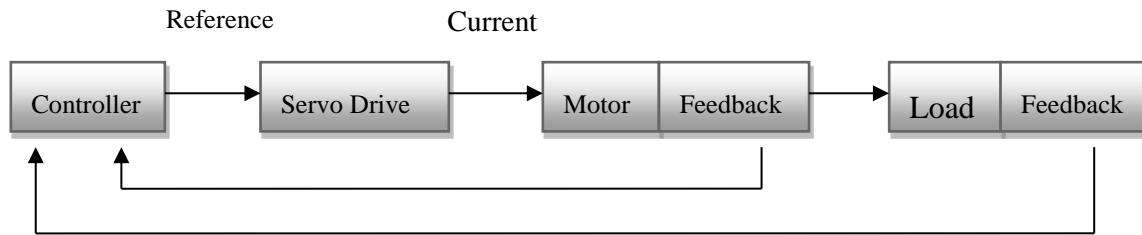


Figure 5.1: Overall schematic of force feedback system

Figure 5.1 shows the components used in a servo system to control the position, velocity or acceleration of the motor.

5.1 PWM generation

The drive represents the electronic power converter that drives the motor according to the controller reference signals. There exist a lot of ways to amplify the electrical signals; Pulse Width Modulation (PWM) is the most efficient approach. The PWM servo drive is a current loop circuit that controls the output current by varying the duty cycle of the output power stage. The PWM current control circuit is shown in Figure 5.2.

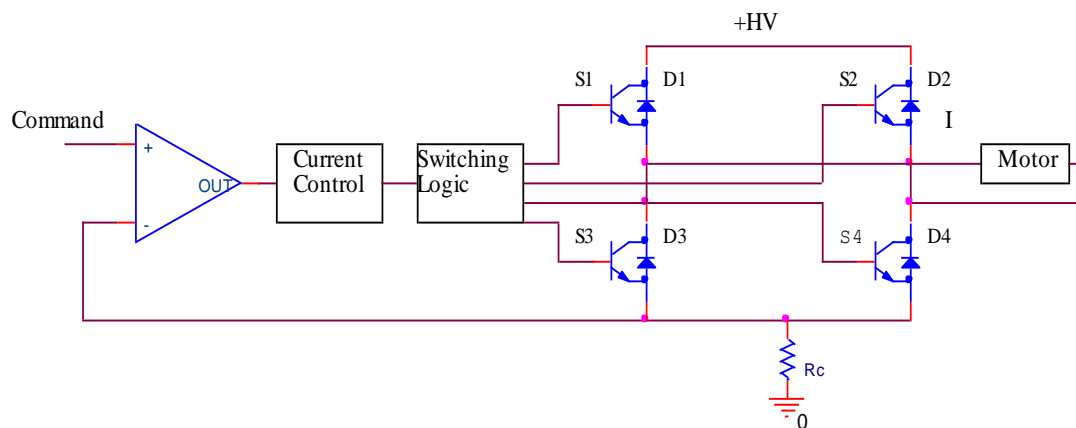


Figure 5.2: PWM Current control circuit

The diodes shown in Figure 5.2 are used to control the current continuity in system and the R_C is used to measure the output current. The transistors (MOSFET or IGBT)

are used to switch on and off the diodes. For instance, when switch S1 and S4 (or S2 and S3) are activated, current will flow in the positive (or negative) direction and increase. When switch S1 is off and S4 is on (or S2 off and S3 on) current will flow in the positive (or negative) direction and decrease (via one of the diodes). The switch “on” time can be computed by the difference between the actual current and demand current. The Current control circuit compares both signals (Actual and demand current) by the switching logic circuit and activate the switches. Overall dependency between the pulse width (on time) and the current pattern is shown in Figure 5.3.

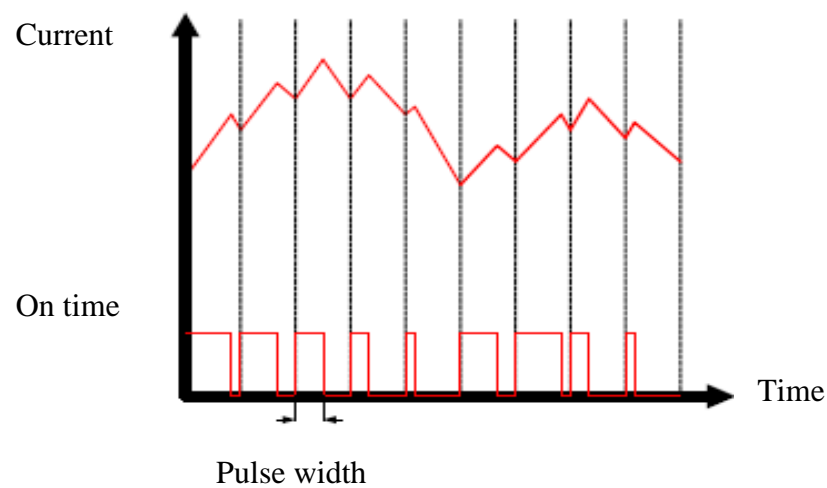


Figure 5.3: Relation of output current and duty cycle [19]

Maxon DC motor 168505 series is used as force feedback actuator for Chalmers driving simulator. Motor current and voltage requirements are computed based on the maximum required torque and velocity respectively. The relations between velocity, torque and power curves are shown in Figure 5.4.

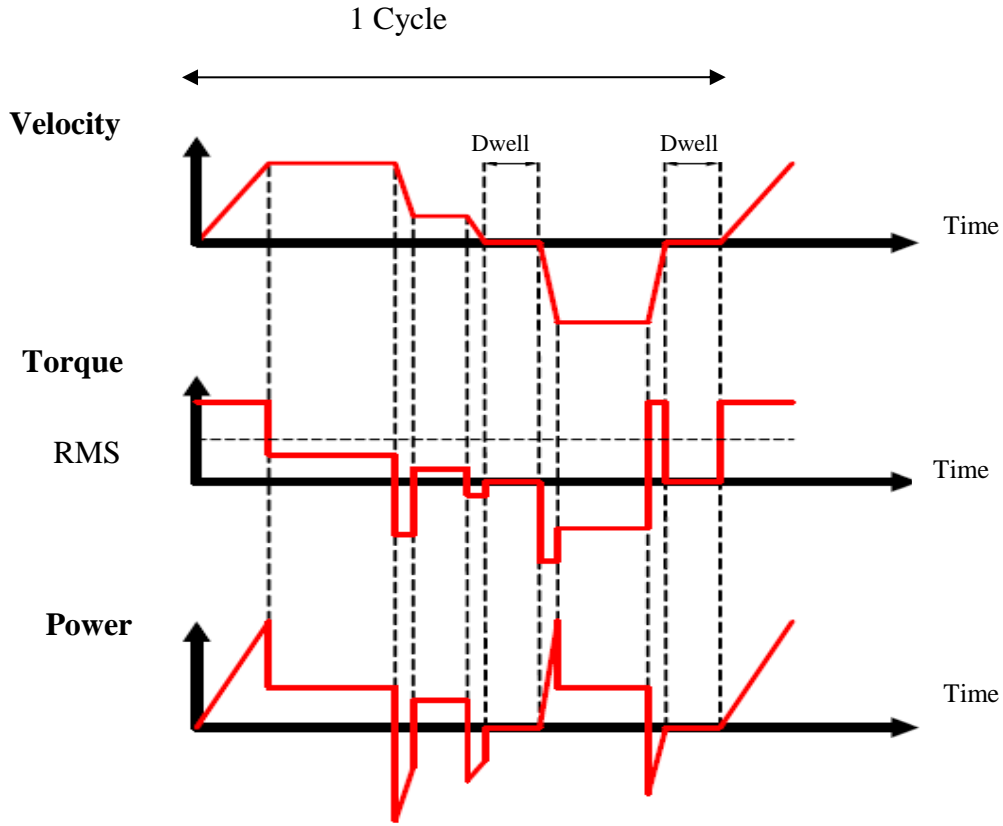


Figure 5.4: Relations between velocity, Torque and power curves [19]

The power is equal to Torque * Speed of the motor. The motor voltage (V_m) and current (I_m) should be chosen where power is maximum. The DC motor current (I_m) in amps is function of the torque needed to move the load, it can be computed as follows:

$$I_M = \frac{\text{Torque}}{K_T} \quad (5.1)$$

where K_T is motor's torque constant. So the motor current is proportional to the motor shaft torque, and the motor voltage is proportional to the motor speed and can be calculated as shown :

$$\begin{aligned} V_m &= R_m \cdot I_m + E \\ E &= K_e \cdot \omega_m \end{aligned} \quad (5.2)$$

where E is the motor back-EMF voltage and K_e is the voltage constant and ω_m is the maximum speed of motor. Figure 5.5 represents transformer is used to transform the

AC, DC voltage will charge the capacitor. The point should be noticed that during braking, most of the stored mechanical energy is fed back into the power supply, which charges the output capacitor to a higher voltage. If the charge reaches the drive's over-voltage shutdown point, motor control and braking cease. To ensure smooth braking of large inertial loads the shunt regulator is used. Thereby, when the DC bus reaches the shunt voltage of the shunt regulator, the voltage comparator unit turns on the electronic switch, which connects the R (47Ω) power resistor across the DC bus which dissipates the energy from the DC bus. After the bus voltage is reduced to less than the shunt voltage setting, the resistor is disconnected from the bus.

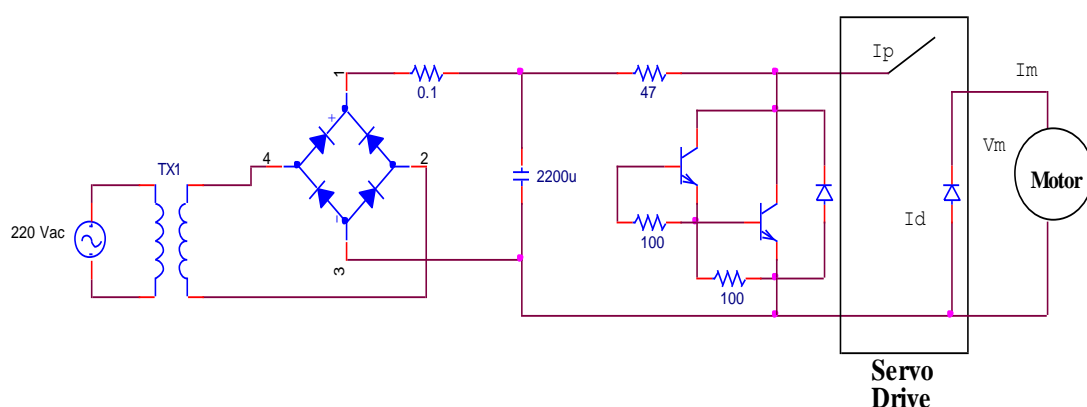


Figure 5.5: Schematic of the motor's power supply and servo drive used for Chalmers simulator

The power supply current is based on the maximum required current by the system which is defined as follows:

$$I_{PS} = \frac{V_M \cdot I_M}{V_{PS} \cdot (0.98)} \quad (5.3)$$

where I_{PS} , V_{PS} are the current and voltage of power supply respectively. Figure 5.6 represents the overall schematic of voltage and current changing for motor, diode and capacitor regarding to the MOSFET switch. The power supply power is approximately equal to drive output power plus 3 to 5%. As shown in, the power supply current is a pulsed DC current, so that when the MOSFET switch is on, the motor current is equal to power supply current; when the MOSFET is off, it is zero. Therefore the power supply current is a function of the motor current and PWM duty cycle. As shown in Figure 5.5, the servo drive is located between DC motor and

power supply. The servo drive is used in order to generate the calculated torque (τ_{motor}) which is determined in section 4.2. As mentioned before, the motor's torque and speed are proportional to the motor current and voltage respectively. For this reason, motor's torque and speed are based on the motor controller outputs (Voltage and current). So, the brushed DC motor's torque is controlled by servo

Controller which creates the PWM signals according to the command torque from National Instruments D/A converter. In this project, ADVANCED motion controller 25A8 series is used as motor controller on simulator. The motion control reference command is computed by the model which is created in order to calculate the steering system feedback torque.

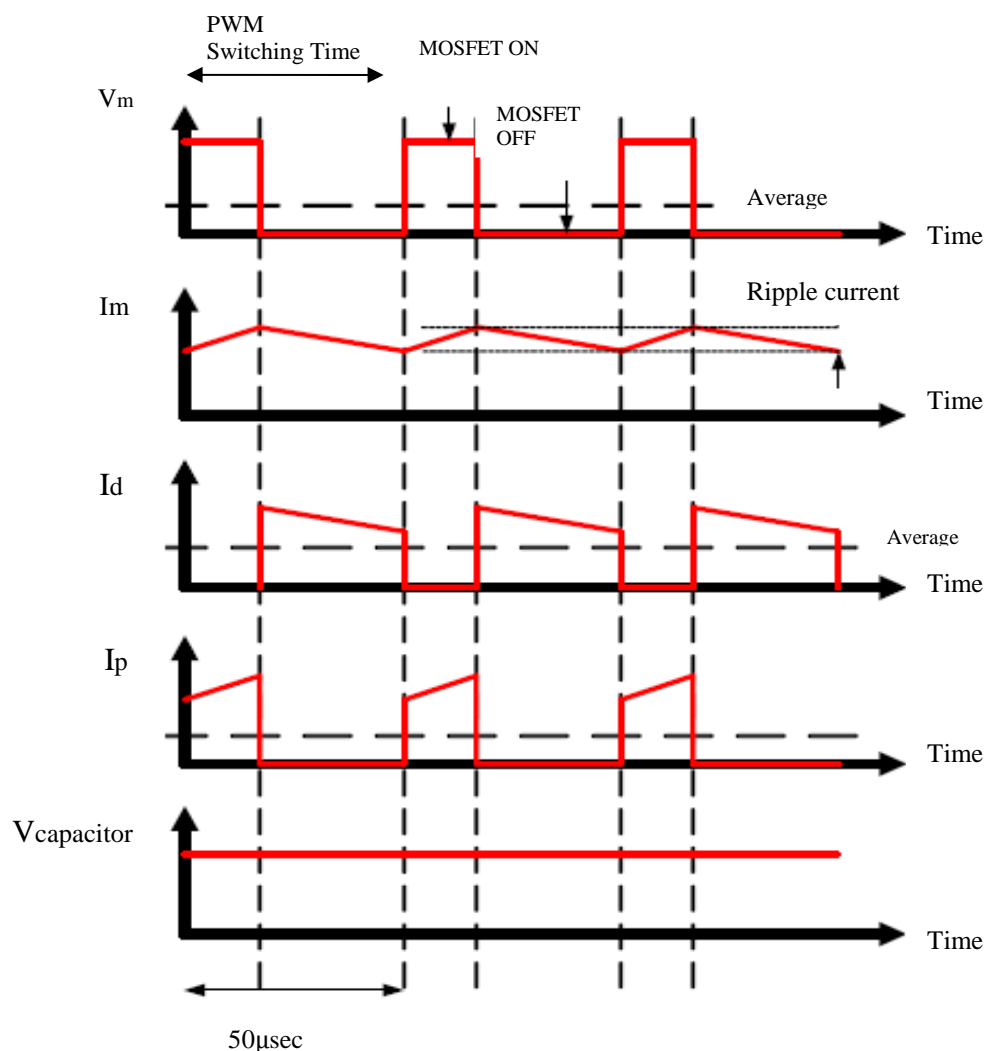


Figure 5.6: Overall schematics of motor inputs and servo drive outputs

5.2 Steering wheel feedback torque command

The developed model of XC90 Volvo computes generated torques by steering system during driving and dictates the steering wheel velocity $\dot{\theta}_{sw}$ constituting the command sent to the velocity control DC motor as follows:

$$\dot{\theta}_{sw} = \int_0^t \frac{\tau_d + \tau_{Lka} + \tau_{assist} - (\tau_{align} + \tau_f + \tau_{speed} + b_s \cdot \dot{\theta}_{sw})}{J_s} d\tau \quad (5.4)$$

where τ_d is the torque applied by driver, τ_{Lka} is the lane keeping assistance which is determined in section 4.2. τ_{align} is the self-aligning torque which is computed in section 3.2.2.

τ_f is the torque caused by the friction of steering system which is determined in section 3.3. The b_s is the steering column damper and J_s is the steering wheel moment of inertia. τ_{speed} represents a feedback torque which is a product of speed stiffness term K_s , the longitudinal velocity V_x and steering wheel angle θ_{sw} . The τ_{speed} can be determined as follows:

$$\tau_{speed} = K_s \cdot V_x \cdot \theta_{sw} \quad (5.5)$$

The electric noise sampled from the A/D board with the DC motor illustrates the undesired noise when the motor is enabled. So, first order low-pass Butterworth active filtering is used to reduce the noise for the sensors in the model. On the other hand, the command signals from D/A board need to amplify. In order to amplify the reference command the difference amplifier is used for command signals. The schematic of the difference amplifier and second order low-pass filter are shown in Figure 5.7.

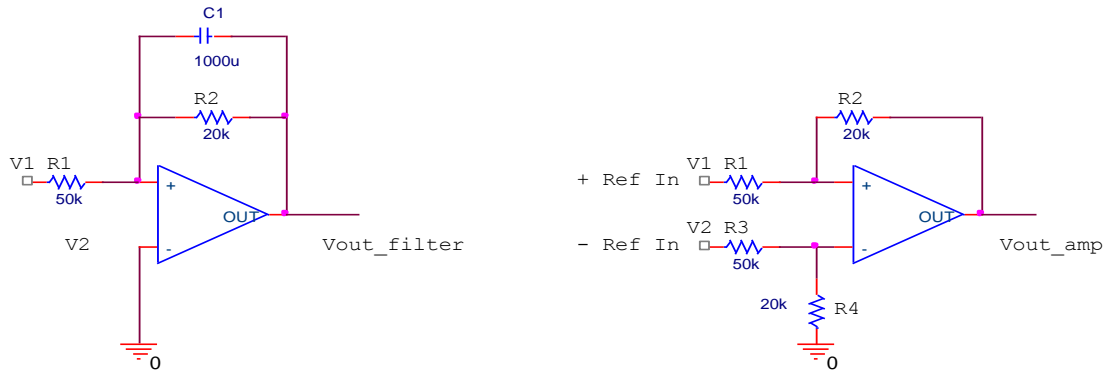


Figure 5.7: First order low-pass filter (left) and difference amplifier (right)

where V_{out_filter} and V_{out_amp} can be calculated as follows:

$$V_{out_amp}(s) = \frac{R_2}{R_1} (V_2(s) - V_1(s)) \quad (5.6)$$

$$V_{out_filter}(s) = \frac{1}{sR_2C_1 + 1} V_1(s) \quad (5.7)$$

In this section some information in related to the implementation of force feedback torque on driving simulator has been provided.

.

6. MODEL VALIDATION

Model validation for this project is divided into two parts: the first part is included the vehicle dynamics model validation and the second part is the lane keeping assistance system validation. The vehicle dynamics model validation procedure done by comparison with XC 90 Volvo measurement data. The proposed lane keeping assistance system has been validated by testing the function activity in the driving simulator. The vehicle dynamics model parameters are tuned to reduce the difference between matching of the measurement data from Volvo and to increase the drivability in the Chalmers driving simulator.

6.1 Model comparison with measurement data

The measurement data from Volvo were available in three maneuvers. In the following sections only the significant parameters which are developed within the project are represented. The extracted measurement data are recorded in quick transient maneuvers. Note that the time sample of measurement data and developed model were not match. The time sample of measurement data was 20ms while the sample time of model was 1ms. In order to fix this problem, the model parameter regarding to the measurement data time sample is selected. The transient response of the vehicle can be evaluated by driving car at constant speed in a straight direction, where sinusoidal steering wheel inputs of different frequencies applied (0.2-2.5 Hz). Thus the validation of the lateral velocity and acceleration would be feasible to determine it in the open-loop test method, since the lateral force of tire is function of the lateral acceleration. In the first part, the developed model will be compared by the measurements data at 81km/h or 22.5 m/s. The steering wheel input to the model and measurement data are shown in Figure 6.1.

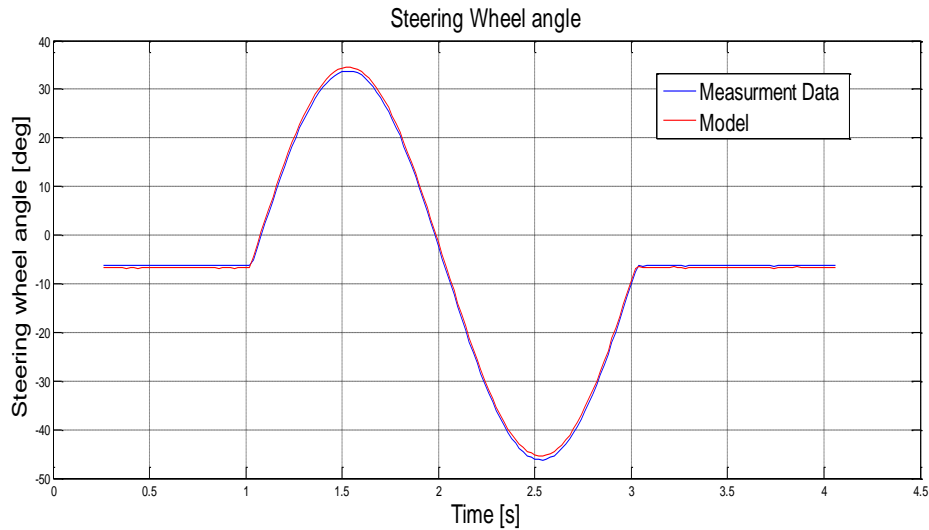


Figure 6.1: Steering wheel angles, at 81Km/h

In order to evaluate the model, the steering wheel angle measured from measurement data is used as input to the model.

The steering wheel response is mainly related to the steering system forces such as: forces on tires and rack-pinion. Self-aligning torque has important role in steering response.

During this project the self aligning torque of the previous model is developed regarding to the caster and kingpin angle effect. The tire's self-aligning torque is function of lateral force of front tires, the lateral torque of front left and right tires are shown in Figure 6.2 and 6.3 respectively.

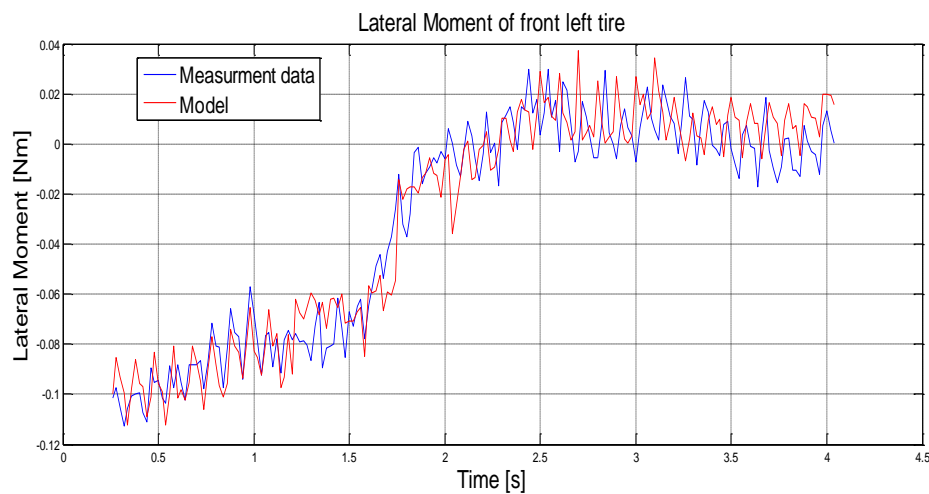


Figure 6.2: Transient response of lateral moment for front left tire, at 81Km/h

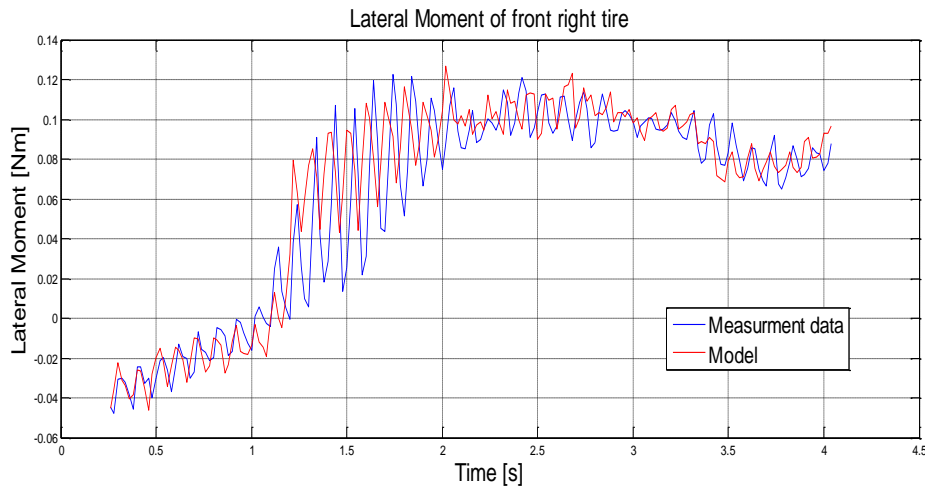


Figure 6.3: Transient response of lateral moment for front right tire, at 81Km/h

The self-aligning torque is the torque that tire creates around the vertical axis when it rolls along. The magnitude of the self-aligning torque can be determined as the product of the lateral force and the lateral offset of tire due to the kingpin and caster angle of the steering axis.

6.2 Tests for evaluating the Steering response in driving simulator

A double lane change maneuver is a widely established test method to study vehicle dynamics behavior and vehicle safety tests in extreme conditions. In this maneuver, the driver is allowed to follow the cone track at the prescribed speed, whereby driver is allowed to adjust the acceleration pedal position to keep a constant speed.

Regarding to aim of this project, it is the necessity to understand how far from reality is the developed model in terms of steering response. This part is related with steering feel of driver during the maneuver in order to compare the steering feel in the simulator and real car. The second aim is to test the lane-keeping assistant torque efficiency and driver reaction near the road limits.

The tests were performed with 15 volunteers in 3 rides with 3 different models: LKA (Lane Keeping Assistance), PIB (Post Impact Braking), PISC (Post Impact Stability Control). In the end of experiments they have been given 2 series of questions; The first part of questions related to the steering response of the model at low, medium

and high speed turning. The second part of questions are related to lane-keeping assistant function efficiency.

The volunteers were asked to drive the simulator in 3 rides for 2-3 minutes per each ride without knowing what model they were driving. The drivers also had the opportunity to drive 3 models in a double-lane change manoeuvre like the one performed at the test track. The drivers tested 3 different vehicle dynamics models to express their judgment on different speeds; After driving in 3 rides, the drivers filled in a questionnaire, show in Appendix C, they were asked to give a point for each model from 0 to 10. In the following sections the results of these tests are reported. The results described in terms of the mean value obtained by the models at different speeds. The average of the sample which can be calculated from equation 6.1:

$$\bar{S} = \frac{\sum_{i=1}^N S_i}{N} \quad (6.1)$$

The steering feel score of models in different speed is shown in Figure 6.6.

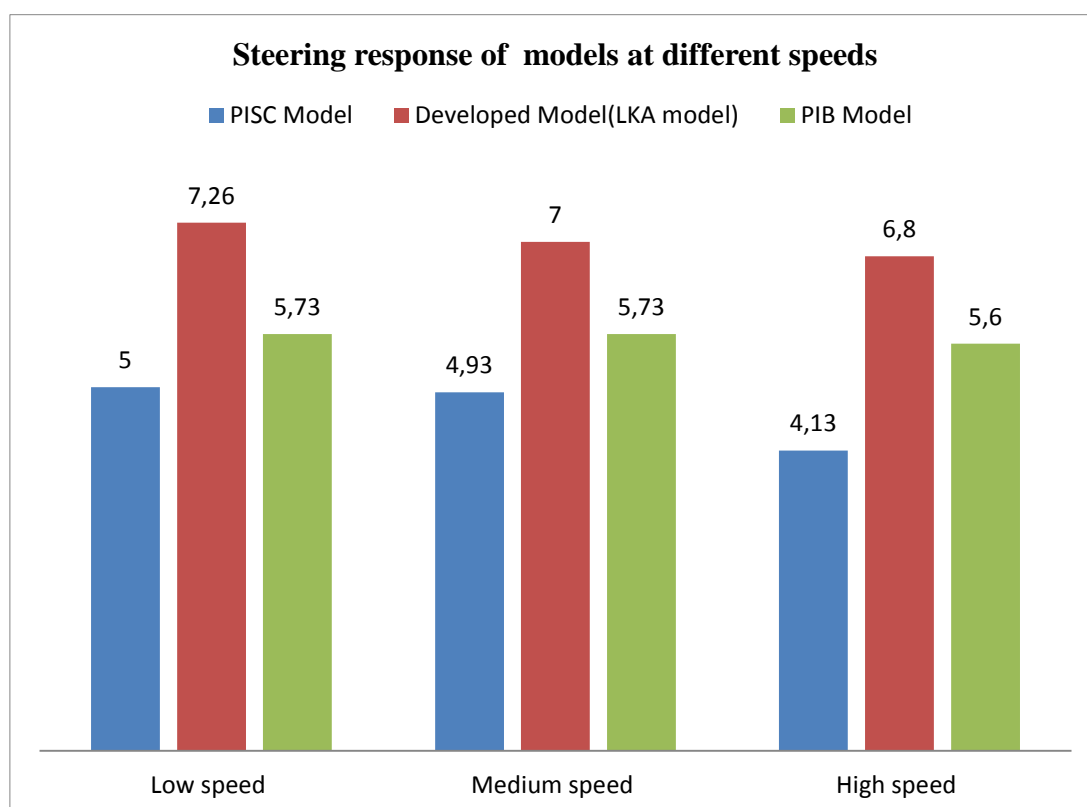


Figure 6.6: Low, medium and high speed steering feel of PISC model (blue), Developed model-LKA model (red) and PIB model (green).

The PIB model has an aligning torque which is more “elastic”, with a high self-aligning-torque and without considering the power steering system. For this reason we asked participants to compare the models in terms of vehicle stability response at high speeds. The PISC model is considered without steering wheel feedback effect.

The developed model (LKA model) appears to be more realistic, with the steering wheel returning in centre position. During the tuning process before experiments, many efforts have been put to tune the effect of regulating friction and power steering assistance on steering wheel force feedback torque.

In questionnaire 1 we also asked participants to give a point (0-10) for simulator stability when steering wheel is turning fast. This question purpose was to determine the vehicle stability response of 3 models when the steering wheel is turning fast. The scores of simulator response stability for 3 models are shown in Figure 6.7.

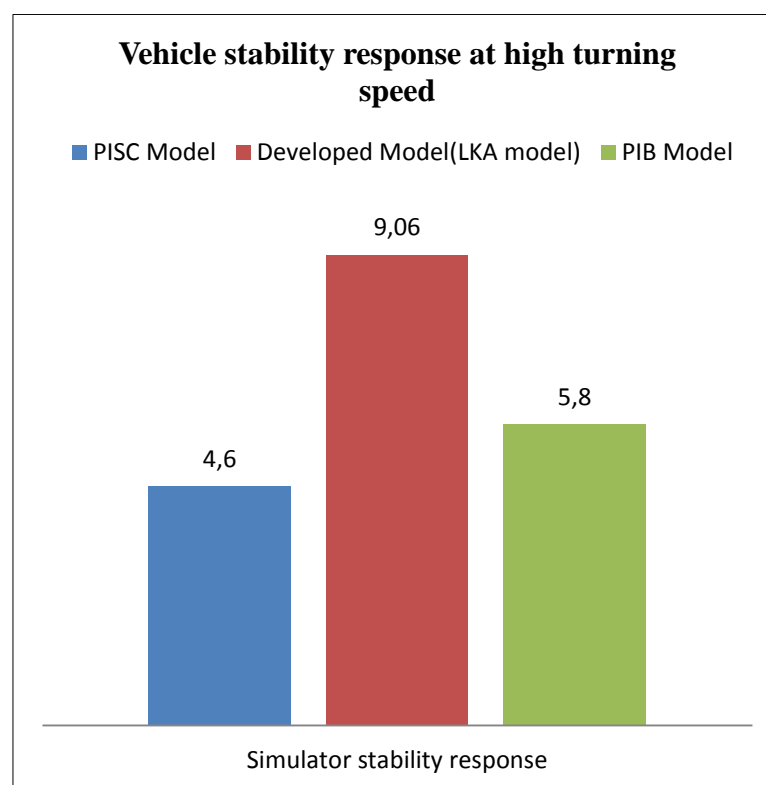


Figure 6.7: High speed vehicle stability response of PISC model (blue), Developed model-LKA model (red) and PIB model (green).

6.3 Tests for evaluating the lane keeping assistance torque functionality in driving simulator

In order to test this function, 15 participants have been asked to drive simulator on a test track. They have not been informed that the LKA system is active in which model. They have been asked to drive in the low speed line of highway at speed more than 75km/h for one minute and cease the steering wheel turning like sleepless position. They have been asked to do the first reaction after alarm sound. The alarm sound was set to activate when the vehicle is close the road limits. This experiments helps us to evaluate the reaction of drivers when they hear the alarm sound and to understand the usefulness of this function for drivers in extreme conditions. Driver's comments must be qualified LKA systems functionality after experiments. Participants have been asked to fill questionnaire1 in related to compare the stability control of vehicle when it is close the road limits. In the questionnaire 2, participants have been asked to explain the first reaction after sound alarm when the vehicle was close the roadsides. Questionnaire 2 contained some question about usefulness of the function.[appendix 3]

One of the questions was related with the first reaction of drivers when they noticed the position of the vehicle near the road limits. The participants have been asked to select between the brake, turning the steering wheel and get lost. The answers of fifteen participants are shown in Figure 6.8.

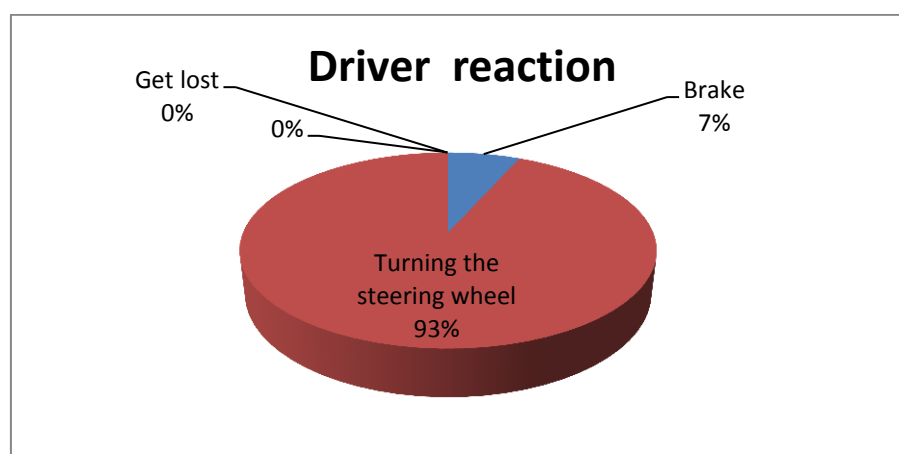


Figure 6.8: The rate of drivers reaction when they noticed the position of the vehicle near the road limits

As Figure 6.8 shows 93% of the drivers turned steering wheel after sound alarm near the road limits.

The scores of simulator stability control after sound alarm and drivers reaction for preventing of road departure are shown in Figure 6.9.

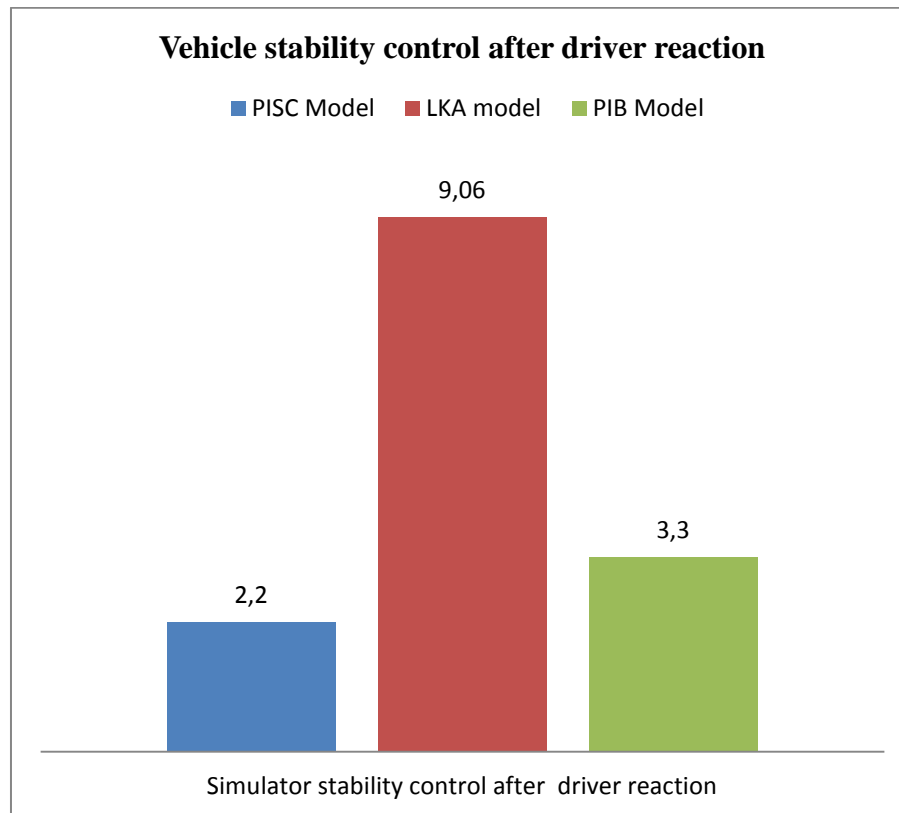


Figure 6.9: Vehicle stability control after driver reaction for PISC model (blue), LKA model (red) and PIB model (green).

The following Figure represents LKA functionality gathered by the statistical tests done by the participants (The functionality quantifie how much LKA helps to keep vehicle between the road limits).

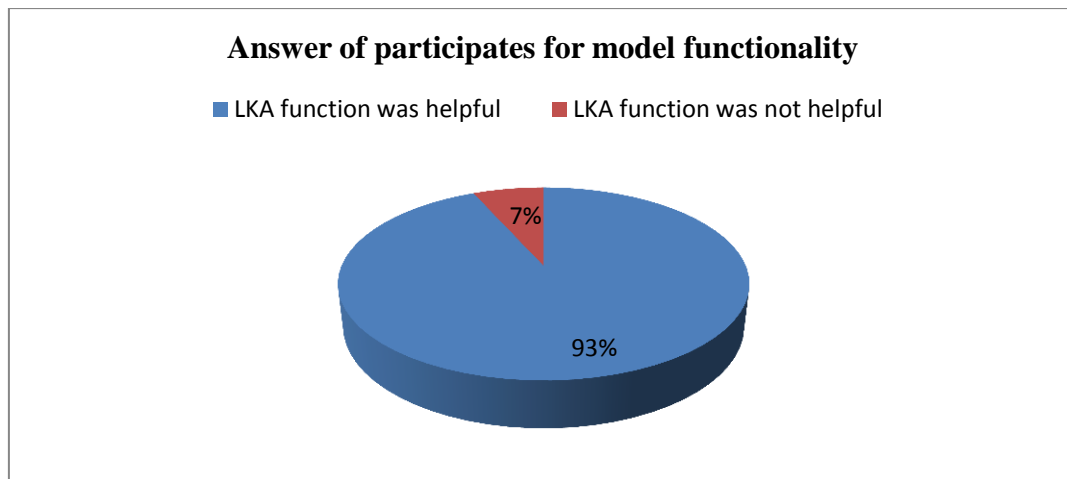


Figure 6.10 The opinion of participates in terms of usefulness of the LKA model

As Figure 6.10 shows, 93% of participates believed that the LKA model is useful to keep the vehicle when it is close to roadside limits.

7. CONCLUSION

The main conclusions obtained in this master thesis was the development of the steering wheel force feedback with focus on LKA in Chalmers driving simulator. The steering wheel force feedback concerns to improvement in two area:

- development of steering wheel feedback torque to improve the steering feel of driver in driving simulator
- verification of derived lane-keeping assistance function by adding the calculated LKA torque to steering wheel feedback torque and test in Chalmers driving simulator

The model has been developed using Matlab[®]/Simulink[®] as programming language and it has been validated both with a comparison versus measurements data (coming from Volvo) and with simulations performed in the Chalmers simulator.

The LKA model can be seen as an evolution of XC 90 Volvo vehicle dynamics model which is currently used in the Chalmers simulator. This model uses a closed-loop control system to keep the vehicle in road limits regarding the lateral offset and heading error between the vehicle's COG and the road centerline. This function reduces the lateral offset of vehicle by providing the correction wheel angle through the steering wheel torque.

8. RECOMMENDATION AND FUTURE WORK

This chapter consists of some recommendations for future work and further development.

- Deeper study related with the suspension in order to improve vertical behaviour of the vehicle in terms of acceleration and vibrations.
- Improve the powertrain subsystem, to increase the vehicle behaviour for initial acceleration.
- Model the friction of rack as variable in function of the rack displacement.
- Deeper study to model the steering feedback dependency in function of the vehicle speed.
- Improve the audio and the quality graphic of the scenario to provide a better feel for driver.
- Improve the interaction of driver and simulator by adding a touchpanel to the simulator cockpit.

REFERENCES

- [1] **Alirezaei, M., Corno, M., Katzourakis, D., Ghaffari, A., Kazemi, R. (2012).** A Robust Steering Assistance Sysytem for Road Departure Avoidance. *IEEE Transactions on Vehicular Technology*, Vol. 61, No.6, (2012).
- [2] **Benito, G. & Nilsson, H. (2006).** Vehicle Stability Control for Roadside Departure Incidents by Steering Wheel Torque Superposition, *Master's Thesis*, department of Applied Mechanics & Signals and Systems, Chalmers Uninversity of Technology, Göteborg, Sweden.
- [3] **Gómez Fernández, J. (2012).** A Vehicle Dynamic Model for Driving Simulators. *Master's Thesis*, department of Applied Mechanics, division of Vehicle Engineering and Autonomous Systems, Chalmers Univesrity of Technology, Göteborg, Sweden
- [4] **Judy Hsu, Y.H. (2009).** Estimation and Controlof Lateral Tire Forces Using Steering Torque. *PhD. Thesis*, department of mechanical engineering, Stanford University, Stanford, United states of America
- [5] **Katzourakis, D. (2012).** Driver Steering Support Interfaces near the Vehicle's Handling Limit. *PhD. Thesis*, Technische Universiteit Delft, Delft, Netherlands.
- [6] **Kusachov, A., Al Moutamid, F. (2012).** Post Impact Braking Verification in Motion Platform Simulator. *Master's Thesis*, department of Applied Mechanics, division of Vehicl Engineeringand and Autonomous Systems, Vehicle Dynamics Group, Chalmers University of Technology, Göteborg, Sweden.
- [7] **Obialero, E. (2013).** A Refined Vehicle Dynamic Model for Driving Simulators. *Master's Thesis*, department of Applied Mechanics, division of Vehicle Engineering and Autonomous Systems, Chalmers University of Technology, Göteborg, Sweden.
- [8] **Pacejka, H.B. (2005).** Tire and Vehicle Dynamics (2th edition.) SAE International, Englewood Cliffs, New Jersey.
- [9] **Pohl, J. & Ekmark, J. (2007).** SYN3: A Lane Keeping Assist System for Passenger Cars, Design Aspects of the user interfce, *Volvo Car Corporatio Report*, Paper No. 529, Göteborg, Sweden.
- [10] **Rösth, M. (2007).** Hydraulic Power Steering Design in Road Vehicles. Dissertation No. 1068, Division of Fluid and Mechanical Engineering Systems, Department of Mechanical Enginerring, Linköping, Sweden.
- [11] **Sato, K., Goto, T., Kubota, Y., Amno, Y. & Fukui, K. (1998).** A study on a Lane Departure Warning System using a Steering Torque as Warning Signal. In *Proceeding of the International Symposium on Advanced Vehicle Control (AVEC) (1998)*, pp.479-484.

- [12] **Suzuki, K.** (2002). Analysis of drivers steering behaviour during auditory or haptic warnings in lane departure situations. In Proceeding of the International Symposium on Advanced Vehicle Control (AVEC) (2002), pp.243-248.
- [13] **Switkes, J. P.,Rossetter, E. J.,Coe, I. A.&Gerdes, J. C.** (2006). Handweel Force Feedback for Lanekeeping Assistance:Combined Dynamics and Stability. *Jornal of Dynamic System, Measurment and Control*, Vol. 128, pp. 532-542 (2006).
- [14] **Url-1**<<http://www.agcoauto.com>>, date retrieved 30.10.2013.
- [15] **Url-2**< <http://www.mathworks.se/help/physmod/sdl/drive/tire.html>>, date retrieved 20.10.2013.
- [16] **Url-3**< http://www.carbibles.com/steering_bible.html>, date retrieved 20.09.2013.
- [17] **Url-4**< <http://www.discounttiredirect.com/direct/infoAlignment.do>>, date retrieved 21.09.2013.
- [18] **Url-5**< <http://www.bestcoiloverguide.com/coilover-parts/camberplates/> >, date retrieved 10.10.2013.
- [19] **Advanced Motion Controls**, Analog Drives for servo Systems and Hardware Installation manual, 25A8Servo drive datasheet, Date retrieved: 20.10.2013, adress: http://www.a-m-c.com/download/manual/AMC_AnalogDrives_InstallManual.pdf

APPENDICES

APPENDIX A: Steering Geometry

APPENDIX B: TMEasy Tire model

APPENDIX C: The pictures of Chalmers driving simulator and simulator control computers

APPENDIX D: Instruction Paper and *Questionnaire 1, 2*

APPENDIX A

Steering geometry calculates the wheel angle with regarding to the steering wheel angle. Real steerig ration from the XC 90 Volvo is used to calculate the wheel angles in this model. This block is modified to approximate the characteristics of an Ackermann steering system. The steering geometry block can be found in *Vehicle/Steering Geometry* block of Vehicle Dynamics model. It is shown in Figure A.1 also.

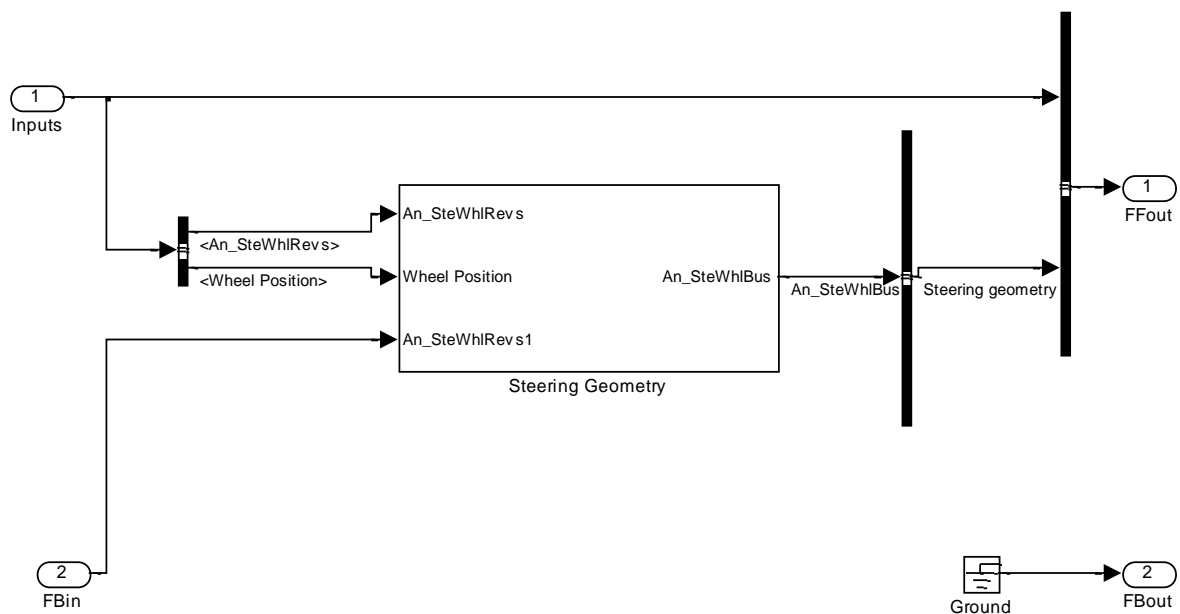


Figure A.1: Steering Geometry sub-system to calculate the wheel angle for each wheel

APPENDIX B

One of the important parts of the vehicle dynamics model is the physical model for tires. This part of vehicle dynamics has an important role in accuracy of final result.

For this reason, everything are related to wheels should be take into account in tire modeling. The TMEasy model was chosen for this project and the main idea behind the model is to characterize the forces vs. slip relation by use the 5 and an optional sixth constant are listed below:

- Slip rate or slip angle for which this maximum force is achieved.
- Maximum force generated by the tire
- Cornering stiffness
- Slip rate or slip angle after considering the full sliding or spinning Condition
- Force generated by the tire at full sliding or spinning situations
- (Optional) Rate of loses force by each tire at higher slip rate or slip angle

The generated slip angle by tire can be calculated from following equations:

$$S = \sqrt{\left(\frac{S_x}{\hat{S}_x}\right)^2 + \left(\frac{S_y}{\hat{S}_y}\right)^2}$$

$$\hat{S}_x = \frac{S_{x_max}}{(S_{x_max})^2 + (S_{y_max})^2} + \frac{\frac{F_{x_max}}{dF_x}}{\sqrt{\left(\frac{F_{x_max}}{dF_x}\right)^2 + \left(\frac{F_{y_max}}{dF_x}\right)^2}} \quad (A.1.1)$$

$$\hat{S}_y = \frac{S_{y_max}}{(S_{x_max})^2 + (S_{y_max})^2} + \frac{\frac{F_{y_max}}{dF_y}}{\sqrt{\left(\frac{F_{x_max}}{dF_x}\right)^2 + \left(\frac{F_{y_max}}{dF_x}\right)^2}}$$

The TMEasy tire model can be found in *Vehicle/Wheels/FL* block of Vehicle Dynamics model. It is shown in Figure A.1 also.

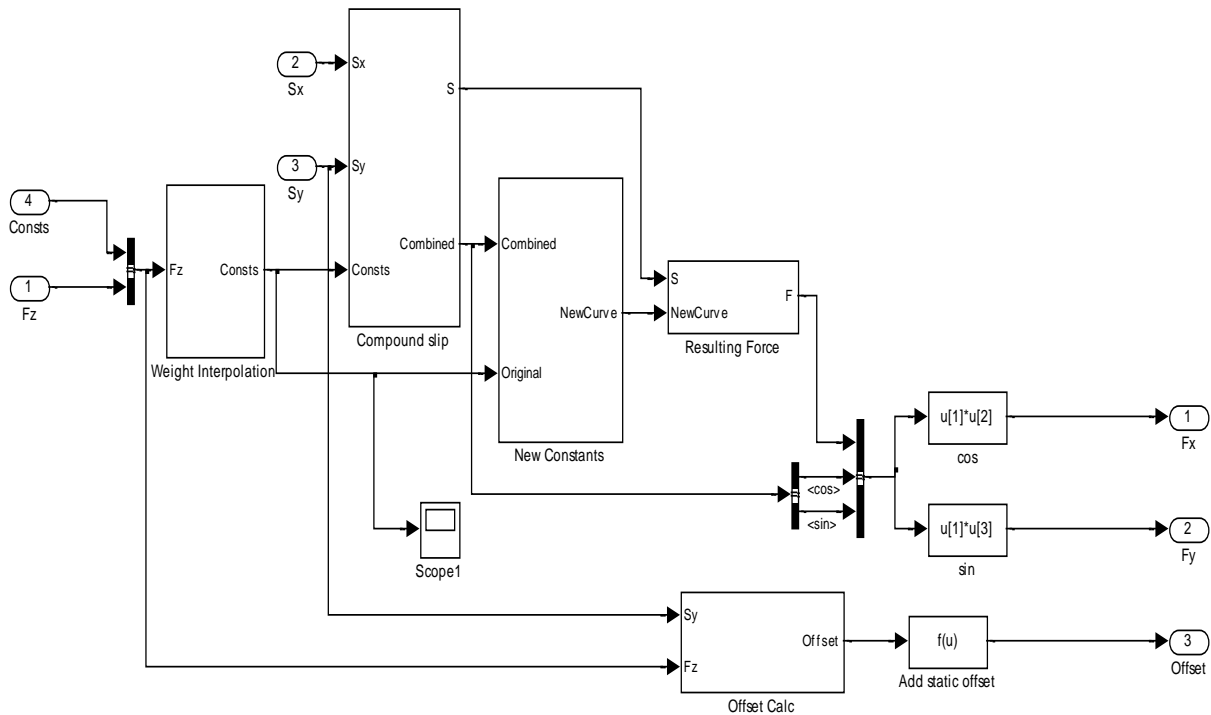


Figure B.1: TMEasy tire model sub-system, to calculate the lateral and longitudinal forces on tires

The More information about TMEasy tire model can be found in [2]

APPENDIX C

In the following section, some pictures of Chalmers driving simulator are shown. This Simulator was used to test the model



Figure C.1: Chalmers driving simulator control computers

The Figure C.1 shows the computers which are used to control the simulator. The middle PC is the Host PC which is described in chapter 1.1.1. The right PC is Kernel and the Left PC is Backup PC.

The Platforms and cockpit of Chalmers driving simulator are shown in Figure C.2.



Figure C.2: Chalmers driving simulator platform and cockpit

Figure C.2 shows the platform and cockpit of the Chalmers driving simulator which is described in chapter 1.1.3.

The Graphical part and screen of Chalmers driving simulator are shown in Figure C.3.



Figure C.3: Graphical screen of Chalmers driving simulator

APPENDIX D

Instruction paper

Hello Dear driver

You are invited to make a test drive on Chalmers Driving simulator in the scope of a Master's Thesis project. This paper will give you a short background and introduction about the ongoing experiment.

The aim of the test is to study the different aspects of the car and driver's behavior, like:

- Test an overall vehicle simulation model (and its separate parts) behavior, especially how well it works with the current steering system.
- Check how realistic the simulator is in both normal driving and limit handling cases.
- Record and analyze the driver's reaction and the vehicle control parameters on the unusual, unforeseen and stressful events.

So the experiment will consist of 3 rides, at the first ride the Model 1 will be run; In the second ride the Model 2 will be test and in the third ride the model 3 will be run. During each ride, you will be given the instruction about the desired driving behavior (like "try to drive with certain speed" or "zigzagging "). Please try to follow the instruction carefully in order to help us to collect the best data set. Try to imagine that you are riding a real car and behave appropriately- avoid collisions, respect the traffic rules and so on.

NOTE: Speedometer has two scales- mph (outer one) and Kph (inner one); we are operating only with Kph.

At the beginning of the experiment, you will be given some 2-3 minutes to drive the simulator in the way you want, so as to feel and test the overall fidelity of the simulator. You can do any braking, steering or combined maneuvers. You will be given a small questionnaire after this ride.

In the end of the experiment you will be given another questionnaire with more specific questions.

NOTE: Everything that you see or feel in the simulator is caused made and sanctioned by us and is part of the experiment!

Please do not worry about the simulator capability. We will inform you to pause in experiment if needed. Please, do not leave the simulator before the platform is parked down.

Also, opening the door of the car will caused the stop of the simulation .So, Please do not open it during the experiment unless you feel a need.

Please, fasten your seat belt before start the simulation and don't change the handbrake position. The Simulator gear is shifting automatically, so you don't need to shift it.

Questionnaire 1

Driver Information

Test Case#: _____

Name: _____

Gender: _____

Driving License: Yes/No _____

Driving Experience: _____ Years

How many km do you drive per year? ☐ 0-10.000 ☐ 10.000-20.000 ☐ More than 20.000

How many times have you used a simulator before? ☐ Never ☐ 1_3 ☐ More than 3

Do you play car related video games? Yes/No

Date and Time of experiment: _____

Model Comparison

How do you perceive the steering response when negotiating low speed turn? (From 0 to10)

Model 1: _____ Model 2: _____ Model 3: _____

How do you perceive the steering response when negotiating medium speed turn? (From 0 to10)

Model 1: _____ Model 2: _____ Model 3: _____

How do you perceive the steering response when negotiating high speed turn? (From 0 to10)

Model 1: _____ Model 2: _____ Model 3: _____

How do you perceive the simulator stability when steering wheel is turning? (From 0 to10)

Model 1: _____ Model 2: _____ Model 3: _____

How do you perceive the simulator stability control for road departure? (From 0 to10)

Model 1: _____ Model 2: _____ Model 3: _____

What should be improved in the models? (Model 1, Model 2, Model 3):

Questionnaire 2

Name: _____

Test case#: _____

Date and time: _____

Questions:

As you probably noticed, at one part of experiments you had an assistance torque to keep the vehicle between the roadsides. The real aim of this experiment was to test the Lane-keeping assistance torque we derived. This function partly takes the control of the vehicle path near the road limits when the driver doesn't have any reaction to avoid of road departure.

So now, knowing all the background if you don't have any question, please answer these questions:

1. Can you describe briefly the unusual events when the vehicle is near the road limits (Alarm, assistance torque)?
2. How did you react when you noticed the position of the vehicle near the road limits (Brake? turning the steering? Get lost?)
3. If you knew about the existing this function, would you react differently?

4. Are you satisfied with your reaction on road departure position?
5. On which side of road limits did you feel the assistance torque?
6. Do you think this function helped you? Why?

Additional Comments (thoughts, suggestions, etc):

Thanks in advance for your participation in these experiments.